

Hadronic cross section of e^+e^- annihilation at bottomonium energy region

Xiang-Kun Dong,^{2,3,*} Xiao-Hu Mo,^{1,3,†} Ping Wang,^{1,‡} and Chang-Zheng Yuan^{1,3,§}

¹*Institute of High Energy Physics, Chinese Academy of Sciences, Beijing 100049, China*

²*Institute of Theoretical Physics, Chinese Academy of Sciences, Beijing 100190, China*

³*University of Chinese Academy of Sciences, Beijing 100049, China*

(Dated: June 24, 2020)

Abstract

The Born cross section and dressed cross section of $e^+e^- \rightarrow b\bar{b}$ and the total hadronic cross section in e^+e^- annihilation in the bottomonium energy region are calculated based on the R_b values measured by the BaBar and Belle experiments. The data are used to calculate the vacuum polarization factors in the bottomonium energy region, and to determine the resonant parameters of the vector bottomonium(-like) states, $Y(10750)$, $\Upsilon(5S)$, and $\Upsilon(6S)$.

PACS numbers: 13.66.Bc, 13.25.Gv, 14.40.Rt

*Electronic address: dongxiangkun14@mailsucas.edu.cn

†Electronic address: moxh@ihep.ac.cn

‡Electronic address: wangp@ihep.ac.cn

§Electronic address: yuancz@ihep.ac.cn

I. INTRODUCTION

The cross section of e^+e^- annihilation into hadrons is essential information for Quantum Electrodynamics (QED) as it is related to the vacuum polarization (VP) of the photon propagator. The measurement of these cross sections is one of the important topics in various e^+e^- colliders from low to high energy, and the precision of the measurements has been successively improved since the running of the first generation of e^+e^- colliders [1]. The data have been used in many calculations involving the photon propagator, especially in the high precision calculations of the anomalous magnetic moment of the μ , a_μ , and the running of the fine structure function, $\alpha(s)$, where s is the center-of-mass (CM) energy squared [2–4].

The cross section of e^+e^- annihilation into hadrons is often reported in terms of R value, defined as

$$R = \frac{\sigma^B(e^+e^- \rightarrow \text{hadrons})}{\sigma^B(e^+e^- \rightarrow \mu^+\mu^-)}, \quad (1)$$

where $\sigma^B(e^+e^- \rightarrow \mu^+\mu^-) = \frac{4\pi\alpha^2(0)}{3s}$, is the Born cross section of $e^+e^- \rightarrow \mu^+\mu^-$. The experimental measurements of the R values are compiled in Ref. [1]. There are many data at low energies ($\sqrt{s} < 2$ GeV) with precision at 1% level; while the measurements are sparse and less precise at higher energies, for example, the charmonium ($3.7 < \sqrt{s} < 5.0$ GeV) and the bottomonium ($10.5 < \sqrt{s} < 11.2$ GeV) energy regions. One of the reasons of less measurements at high energy is the smaller contribution to the VP, and another reason is the fact that fewer experiments were designed in these energy regions.

The cross sections of $e^+e^- \rightarrow b\bar{b}$ were measured in much higher precision by BaBar [5] and Belle [6] experiments in the bottomonium energy region, i.e., $\sqrt{s} = 10.5$ to 11.2 GeV, than by CUSB [7] and CLEO [8] experiments more than 30 years ago. However, neither BaBar nor Belle (let alone CUSB and CLEO) did radiative corrections to the measured cross sections, so the data cannot be used directly for many calculations where the Born cross sections are needed as input.

In this paper, we describe how to get the Born cross section based on the published data from the BaBar and Belle experiments with some reasonable assumptions. We report the Born cross sections from these experiments and discuss the usage of the data samples in the calculation of the VP factors especially in the bottomonium energy region, and the fit to the dressed cross sections to extract the resonant parameters of the vector bottomonium states. We also discuss a possible determination of the VP directly by measuring $e^+e^- \rightarrow \mu^+\mu^-$ cross sections with high luminosity data at the Belle or Belle II experiment, and a strategy to search for the production of invisible particles in e^+e^- annihilation.

II. RADIATIVE CORRECTION

The experimentally observed cross section (σ^{obs}) is related to the Born cross section via

$$\sigma^{\text{obs}}(s) = \int_0^{x_m} F(x, s) \frac{\sigma^B(s(1-x))}{|1 - \Pi(s(1-x))|^2} dx, \quad (2)$$

where σ^B is the Born cross section, $F(x, s)$ has been calculated in Refs. [9–11] and $\frac{1}{|1 - \Pi(s)|^2}$ is the VP factor; the upper limit of the integration $x_m = 1 - s_m/s$, where $\sqrt{s_m}$ is the experimentally

required minimum invariant mass of the final state f after losing energy to multi-photon emission. In this paper, $\sqrt{s_m}$ corresponds to the $B\bar{B}$ mass threshold, which is 10.5585 GeV.

The radiator $F(x, s)$ is usually expressed as [9]

$$F(x, s) = x^{\beta-1} \beta \cdot (1 + \delta') - \beta(1 - \frac{1}{2}x) + \frac{1}{8}\beta^2 \left[4(2-x) \ln \frac{1}{x} - \frac{(1+3(1-x)^2)}{x} \ln(1-x) - 6 + x \right], \quad (3)$$

with

$$\delta' = \frac{\alpha}{\pi} \left(\frac{\pi^2}{3} - \frac{1}{2} \right) + \frac{3}{4}\beta + \beta^2 \left(\frac{9}{32} - \frac{\pi^2}{12} \right), \quad (4)$$

and

$$\beta = \frac{2\alpha}{\pi} \left(\ln \frac{s}{m_e^2} - 1 \right). \quad (5)$$

Here the conversion of soft photons into real e^+e^- pairs is included.

The Born cross section is thus calculated from

$$\sigma^B(s) = \frac{\sigma^{\text{obs}}(s)}{(1 + \delta(s)) \cdot \frac{1}{|1 - \Pi(s)|^2}}, \quad (6)$$

where $(1 + \delta(s))$ is the initial state radiation (ISR) correction factor.

It is obvious that both $(1 + \delta(s))$ and $\frac{1}{|1 - \Pi(s)|^2}$ depend on the Born cross section from threshold up to the CM energy under study, while the Born cross section is the quantity we want to measure. These two factors can only be obtained using the measured quantities with an iteration procedure.

The pure ISR correction factor $(1 + \delta(s))$ depends only on the line shape of $e^+e^- \rightarrow b\bar{b}$ cross section, while $\frac{1}{|1 - \Pi(s)|^2}$ depends also on the R values in the full energy range, we use a two-step procedure to get the Born cross sections.

A. ISR correction factor

The ISR correction factor is obtained with an iterative procedure, following Ref. [12], via

$$\sigma_{i+1}^{\text{obs}}(s) = \int_0^{x_m} F(x, s) \sigma_i^{\text{dre}}(s(1-x)) dx, \quad (7)$$

$$\frac{1}{1 + \delta_{i+1}(s)} = \sigma_i^{\text{dre}}(s) / \sigma_{i+1}^{\text{obs}}(s), \quad (8)$$

$$\sigma_{i+1}^{\text{dre}}(s) = \frac{1}{1 + \delta_{i+1}(s)} \sigma_{i+1}^{\text{obs}}(s) \quad (9)$$

where $\sigma^{\text{dre}}(s) = \frac{\sigma^B(s)}{|1 - \Pi(s)|^2}$ is the dressed cross section. At the zeroth step of the iteration, the observed cross sections are inserted into the integral, playing the role of the dressed cross sections, i.e. $\sigma_0^{\text{dre}}(s) = \sigma^{\text{obs}}(s)$. The iteration is continued until the difference between the two consecutive results is smaller than a given upper limit. The result from the last iteration, denoted by $(1 + \delta_f(s))$, is regarded as the final ISR correction factor.

B. Vacuum polarization factor

A similar procedure is used to calculate the VP factor in the bottomonium energy region. In this calculation, however, the total hadronic cross section is used rather than that of $e^+e^- \rightarrow b\bar{b}$ only. Moreover, instead of depending on the hadronic cross sections in the bottomonium energy region, the VP factor depends on the R values in the full energy region. In addition, there is also contribution from leptons. The VP factor includes two terms [13]

$$\Pi(s) \equiv \sum_{j=e, \mu, \tau} \Pi_l(s, m_j^2) + \Pi_h(s). \quad (10)$$

The first term is the contribution from the leptonic loops with

$$\Pi_l(s, m^2) = \Pi_R + i \Pi_I \quad (11)$$

for lepton with mass m . For $0 \leq s < 4m^2$, we define $a = (4m^2/s - 1)^{1/2}$,

$$\begin{aligned} \Pi_R &= -\frac{\alpha}{\pi} \left[\frac{8}{9} + \frac{a^2}{3} - 2 \left(\frac{1}{2} + \frac{a^2}{6} \right) \cdot a \cdot \cot^{-1}(a) \right], \\ \Pi_I &= 0, \end{aligned} \quad (12)$$

while for $s \geq 4m^2$, we define $a = (1 - 4m^2/s)^{1/2}$ and $b = (1 - a)/(1 + a)$,

$$\begin{aligned} \Pi_R &= -\frac{\alpha}{\pi} \left[\frac{8}{9} - \frac{a^2}{3} + \left(\frac{1}{2} - \frac{a^2}{6} \right) \cdot a \cdot \ln b \right], \\ \Pi_I &= -\frac{a\alpha}{3} \left(1 + \frac{2m^2}{s} \right). \end{aligned} \quad (13)$$

The second term in Eq. (10) is the contribution from the hadronic loops. This quantity $\Pi_h(s)$ is related to the total cross section $\sigma(s)$ of $e^+e^- \rightarrow$ hadrons in the one-photon exchange approximation through a dispersion relation

$$\Pi_h(s) = \frac{s}{4\pi^2\alpha} \int_{4m_\pi^2}^{\infty} \frac{\sigma(s')}{s - s' + i\epsilon} ds'. \quad (14)$$

Using the identity

$$\frac{1}{x + i\epsilon} = P \frac{1}{x} - i\pi\delta(x),$$

we have

$$\Pi_h(s) = -\frac{s}{4\pi^2\alpha} P \int_{4m_\pi^2}^{\infty} \frac{\sigma(s')}{s' - s} ds' - i \frac{s}{4\pi\alpha} \sigma(s). \quad (15)$$

We follow the procedure in Ref. [14] to calculate the first term in the above equation. First, the integration is performed analytically for narrow resonances J/ψ , $\psi(3686)$, $\Upsilon(1S)$, $\Upsilon(2S)$, and $\Upsilon(3S)$. Second, for the high energy part, it is assumed that $R(s) = R(s_1)$ is a constant above a certain value s_1 . And third, the integral between threshold and s_1 is carried out numerically after separation of the principle value part. Thus we have

$$\begin{aligned} \Re \Pi_h(s) &= \frac{3s}{\alpha} \sum_j \frac{\Gamma_{e^+e^-}^j}{M_j} \frac{s - M_j^2}{(s - M_j^2)^2 + M_j^2 \Gamma_j^2} + \frac{\alpha}{3\pi} R(s_1) \ln \left| \frac{s - s_1}{s_1} \right| \\ &\quad - \frac{s}{4\pi^2\alpha} \int_{4m_\pi^2}^{s_1} \frac{\sigma_{\text{nr}}(s') - \sigma_{\text{nr}}(s)}{s' - s} ds' - \frac{s\sigma_{\text{nr}}(s)}{4\pi^2\alpha} \ln \left| \frac{s_1 - s}{4m_\pi^2 - s} \right|, \end{aligned} \quad (16)$$

where Γ_j , $\Gamma_{e^+e^-}^j$, and M_j denote total width, partial width to e^+e^- pair, and mass of the resonance j , respectively. Here, $\sigma_{\text{nr}}(s)$ is the $\sigma(s)$ in Eq. (15) with the contributions from narrow resonances subtracted.

We use experimental measurements or theoretical calculations of R values in different energy regions in the calculation of the VP factors:

1. For $2m_\pi < \sqrt{s} < 0.36$ GeV, we consider $e^+e^- \rightarrow \pi^+\pi^-$ only, with the π form factor obtained through [15]

$$F_\pi(s) = 1 + \frac{1}{6}\langle r^2 \rangle_\pi s + c_1 s^2 + c_2 s^3, \quad (17)$$

where $\langle r^2 \rangle_\pi = 0.429$, $c_1 = 6.8$, and $c_2 = -0.7$.

2. For $0.36 < \sqrt{s} < 2.0$ GeV, we used R values from PDG compilation [1, 16].
3. For $3.7 < \sqrt{s} < 5.0$ GeV, we use R values from the BES collaboration [17, 18].
4. For $10.5585 < \sqrt{s} < 11.2062$ GeV, we use the R_b values provided by the Belle and BaBar collaborations [5, 6] with proper handling of the ISR correction and VP correction described below.
5. For all the other energy regions, we use R values from pQCD calculation [16, 19]

$$R_{\text{QCD}}(s) = R_{\text{EW}}(s)[1 + \delta_{\text{QCD}}(s)], \quad (18)$$

where $R_{\text{EW}}(s) = 3\sum_q e_q^2$ is the purely electroweak contribution neglecting finite-quark-mass corrections with e_q the electric charges of the quarks; the QCD correction factor is given by

$$\delta_{\text{QCD}}(s) = \sum_{i=1}^4 c_i \left[\frac{\alpha_s(s)}{\pi} \right]^i, \quad (19)$$

with parameters defined in Refs. [16, 19].

Replacing pQCD calculations with recent KEDR measurements [20, 21] for \sqrt{s} between 2 and 3.7 GeV gives very similar results in the bottomonium energy region of interest.

In the bottomonium energy region, the dressed cross section of $e^+e^- \rightarrow b\bar{b}$ is denoted by $\sigma_b^{\text{dre}}(s) = \frac{\sigma_b^{\text{B}}(s)}{|1-\Pi(s)|^2} = (1 + \delta_f(s))\sigma^{\text{obs}}(e^+e^- \rightarrow b\bar{b})$ where $\sigma^{\text{obs}}(e^+e^- \rightarrow b\bar{b})$ is the observed cross section provided by the Belle and BaBar collaborations [5, 6], and the Born cross section of $e^+e^- \rightarrow u, d, s, c$ -quarks from the pQCD calculation is denoted by $\sigma_{udsc}^{\text{B}}(s)$. Then $\sigma_0^{\text{B}}(s) = \sigma_{udsc}^{\text{B}}(s) + \sigma_b^{\text{dre}}(s)$ is taken as zeroth order approximation of the Born cross section of $e^+e^- \rightarrow$ hadrons. Together with the Born cross sections in other energy regions we obtain the first order approximation of the VP factor, $\frac{1}{|1-\Pi_1(s)|^2}$, via Eqs. (15) and (16). Then we use $\sigma_i^{\text{B}}(s) = \sigma_{udsc}^{\text{B}}(s) + \sigma_b^{\text{dre}}(s)/\frac{1}{|1-\Pi_i(s)|^2}$, the i th order approximation of $\sigma^{\text{B}}(s)$, to calculate $\frac{1}{|1-\Pi_{(i+1)}(s)|^2}$. We iterate this procedure until $\frac{1}{|1-\Pi_i(s)|^2}$ is stable and take it as the final VP factor $\frac{1}{|1-\Pi_f(s)|^2}$.

C. Born cross section

The final Born cross section of $e^+e^- \rightarrow b\bar{b}$ can then be calculated with Eq. (6) with the ISR correction factor and VP factor calculated above, i.e.,

$$\sigma_b^B(s) = \frac{\sigma^{\text{obs}}(s)}{(1 + \delta_f(s)) \frac{1}{|1 - \Pi(s)|_f^2}}. \quad (20)$$

III. THE DATA

Both BaBar [5] and Belle [6] experiments measured R_b in the bottomonium energy region:

$$R_b \equiv \frac{\sigma(e^+e^- \rightarrow b\bar{b})}{\sigma^B(e^+e^- \rightarrow \mu^+\mu^-)},$$

where the denominator is the Born cross section of $e^+e^- \rightarrow \mu^+\mu^-$. In both experiments, neither ISR correction, nor the VP correction was considered, so the reported R_b corresponds to the observed cross section. In both experiments, the contribution of the narrow Υ states from the initial state radiation, i.e., $\Upsilon(1S)$, $\Upsilon(2S)$, and $\Upsilon(3S)$ states can be removed from the data supplied in the papers.

The BaBar measurement [5] was based on data collected between March 28 and April 7, 2008 at CM energies from 10.54 to 11.20 GeV. First, an energy scan over the whole range in 5 MeV steps, collecting approximately 25 pb^{-1} per step for a total of about 3.3 fb^{-1} , was performed. This was then followed by a 600 pb^{-1} scan in the range of CM energy from 10.96 to 11.10 GeV, in 8 steps with non-regular energy spacing, performed in order to investigate the $\Upsilon(6S)$ region. Altogether, there are 136 energy points [5]. In the BaBar paper, the ISR produced narrow Υ states, i.e., $\Upsilon(1S)$, $\Upsilon(2S)$, and $\Upsilon(3S)$ states were included in R_b , but in the data file supplied, their contribution is listed and can be removed from the data.

The Belle measurement [6] was done with the scan data samples above 10.63 GeV at total 78 data points. The data consist of one data point of 1.747 fb^{-1} at the peak $\sqrt{s} = 10.869 \text{ GeV}$; approximately 1 fb^{-1} at each of the 16 energy points between 10.63 and 11.02 GeV; and 50 pb^{-1} at each of 61 points taken in 5 MeV steps between 10.75 and 11.05 GeV. The non-resonant $q\bar{q}$ continuum ($q \in \{u, d, s, c\}$) background is obtained using a 1.03 fb^{-1} data sample taken at $\sqrt{s} = 10.52 \text{ GeV}$. Belle experiment supplied a data file of R_b with the ISR produced $\Upsilon(1S)$, $\Upsilon(2S)$, and $\Upsilon(3S)$ states removed (defined as R'_b in Belle paper [6]).

The BaBar and Belle measurements [5, 6] are shown in Fig. 1. Notice that the definitions of R_b are different in these papers. After removing the ISR contribution of the narrow Υ states from BaBar results, the R_b values and the comparison between the two experiments are shown in Fig. 2. In the following analysis, R_b refers to the results after removing the ISR contribution of the narrow Υ states, R_b^{dre} refers to the dressed cross section after the ISR correction is applied, and R_b^B refers to the Born cross section after the ISR and VP corrections are applied.

We can see from Fig. 2 that Belle results are systematically larger than BaBar measurements. To get the size of the systematic difference, we calculate the ratio between the Belle and BaBar measurements in the energy region covered by both experiments. Figure 2 shows the ratio of the R_b between Belle and BaBar measurements, the ratios are fitted with a constant with a good fit

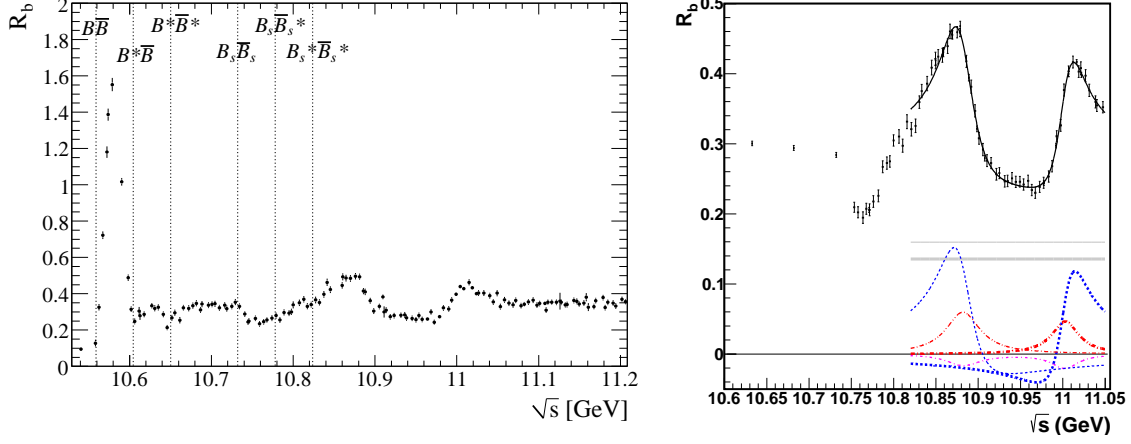


FIG. 1: R_b data from BaBar [5] (left) and Belle [6] (right) experiments. Error bars are statistical only. The curves are the fit described in the original paper.

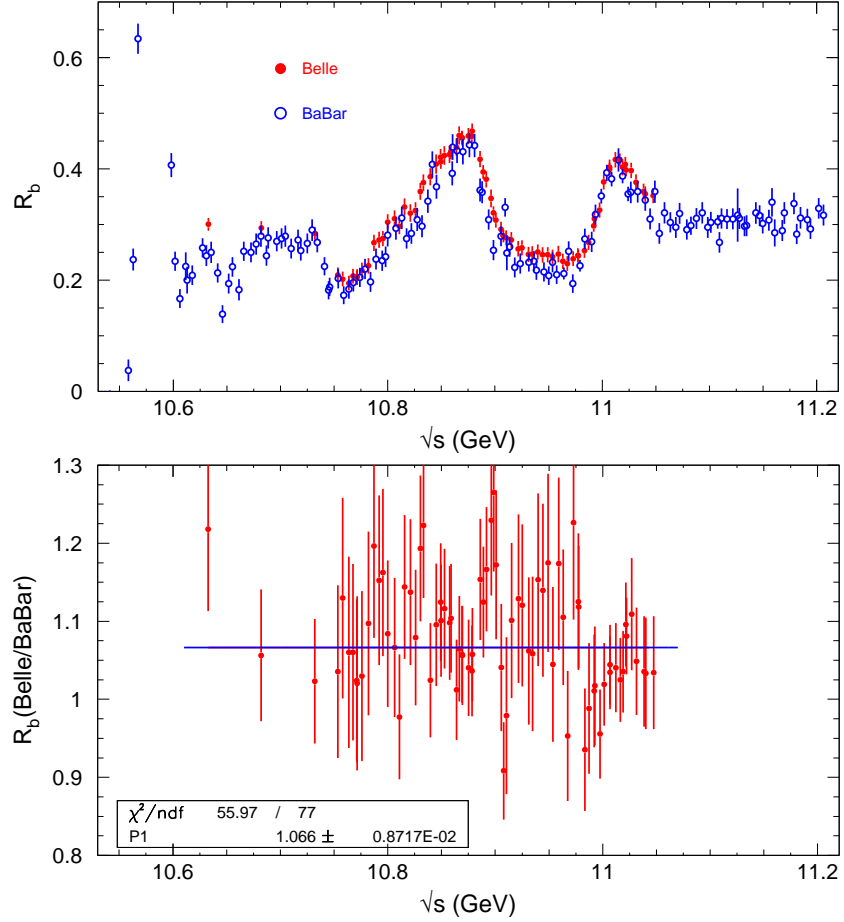


FIG. 2: Comparison of R_b data from BaBar (open cycles) and Belle (Red dots) [top panel] experiments and the ratio of R_b between Belle and BaBar measurements [bottom panel]. Error bars are combined statistical and systematic errors, and the line is a fit to the ratio of Belle and BaBar measurements.

quality, $\chi^2/\text{ndf} = 56/77$, where ndf is the number of degrees of freedom. This indicates that the Belle and BaBar measurements differ by a factor of

$$f = 1.066 \pm 0.009, \quad (21)$$

which is more than 7σ from one if they are the same.

A. Combination of Belle and BaBar data

The BaBar experiment measured the R_b above 11.1 GeV which is very flat. This indicates that the bottomonium resonance region has been passed and the flat continuum region has been reached. At CM energy well above the open-bottom threshold, R values (the total cross section of e^+e^- annihilation) and R_b can be calculated with pQCD with five different flavors of quarks. And this can be compared with the BaBar measurement. If we assume the difference in R_b between Belle and BaBar can be extrapolated to energy region above 11.1 GeV, by comparing the expected Belle measurements in this energy region and the pQCD expectation, we can check the normalization of the Belle data.

To compare R_b with pQCD calculation, ISR correction and VP correction should be applied to the Belle and BaBar measurements since pQCD calculates the Born cross sections. Using the ISR correction factors (point by point correction, average correction factor $1 + \delta \approx 0.901$ above 11.1 GeV) and VP factors ($\frac{1}{|1-\Pi|^2} \approx 1.076$) calculated below, a fit to the R_b^B from BaBar experiment for CM energies between 11.10 and 11.21 GeV yields $R_b^B = 0.316 \pm 0.011$ with the error dominated by the common systematic error.

Assuming Eq. (21) applies to R_b^B at CM energy above 11.1 GeV for Belle measurement, we extrapolate the Belle measurement to this energy region so that we would expect

$$R_b^B = (0.316 \pm 0.011) \times (1.066 \pm 0.009) = 0.337 \pm 0.012. \quad (22)$$

Calculating R_b^B and the total continuum R values from $udsc$ -quarks in pQCD according to Eq. (18), we find that R_b^B is almost a constant for CM energy between 11.10 GeV and 11.21 GeV, which is 0.351 with an uncertainty negligible compared with the experimental measurement; and R_{udsc}^B can be well parameterized as a linear function of CM energy (\sqrt{s} in GeV) between 10 and 12 GeV, i.e.,

$$R_{udsc}^B = 3.5769 - 4.1249 \times 10^{-3} \sqrt{s}. \quad (23)$$

Figure 3 shows the comparison between the BaBar measurements, Belle expected, and the pQCD calculated R_b^B , we can find that Belle data agree with pQCD reasonably well (within about 1σ , the common error of the Belle measurements at high energy is about ± 0.011 , similar to the BaBar measurements) while the BaBar measurements are about 3σ lower than pQCD calculation. As a consequence, we assume BaBar measurement suffers from a normalization bias, and the Belle measurement is normalized properly. In the analysis below, we increase the BaBar measurements by the factor f in Eq. (21) and combine them with the Belle measurements to treat them as a single data set. The normalized and combined data are shown in Fig. 4.

In the remainder of this work, the threshold of open-bottom production is set to be 10.5585 GeV, larger than the first two energy points in BaBar experiment. Therefore, these two data were omitted in our analysis.

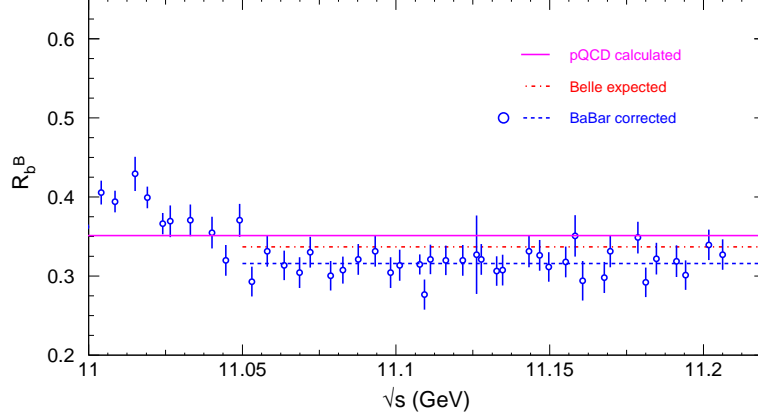


FIG. 3: The R_b^B data from BaBar after ISR and VP corrections (open cycles) and the fit with a constant function (blue dashed line, $R_b^B = 0.316$) and the expected Belle results (Red dash-dotted line, $R_b^B = 0.316 \times 1.066 = 0.337$), and the pQCD calculation (pink line, $R_b^B = 0.351$). Error bars are combined statistical and systematic errors.

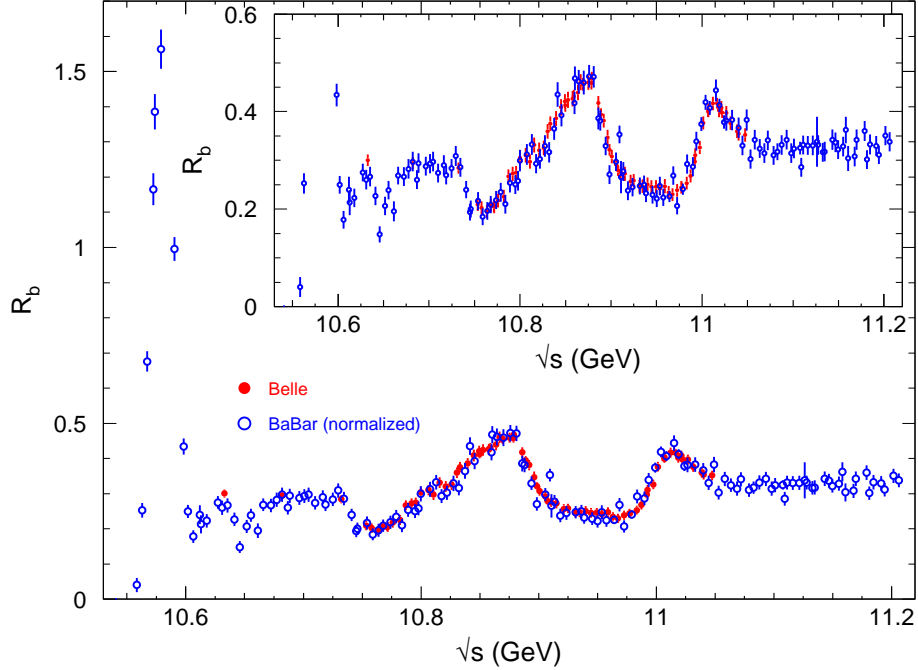


FIG. 4: Normalized R_b data from BaBar (open cycles) and Belle (Red dots), which will be treated as a single data set. Error bars are combined statistical and systematic errors.

B. Parametrization of R_b

To calculate the ISR correction factors, the measured R_b will be used as input. To avoid the point-to-point statistical fluctuation, one may parameterize the line shape with a smooth curve. There is no known function describing the line shape a priori, so one may parameterize the line shape with any possible combination of smooth curves.

We use the “robust locally weighted regression” or “LOWESS” method to smooth the experimental measurements. The principal routine LOWESS computes the smoothed values using the

method described in Ref. [22]. This method works very well only for slowly varying data, which makes the procedure at the $\Upsilon(4S)$ region work improperly. As a consequence, we use the data points directly for $\sqrt{s} < 10.66$ GeV and use the smoothed data for the other data points. Figure 5 shows the smoothed R_b , which looks very reasonable.

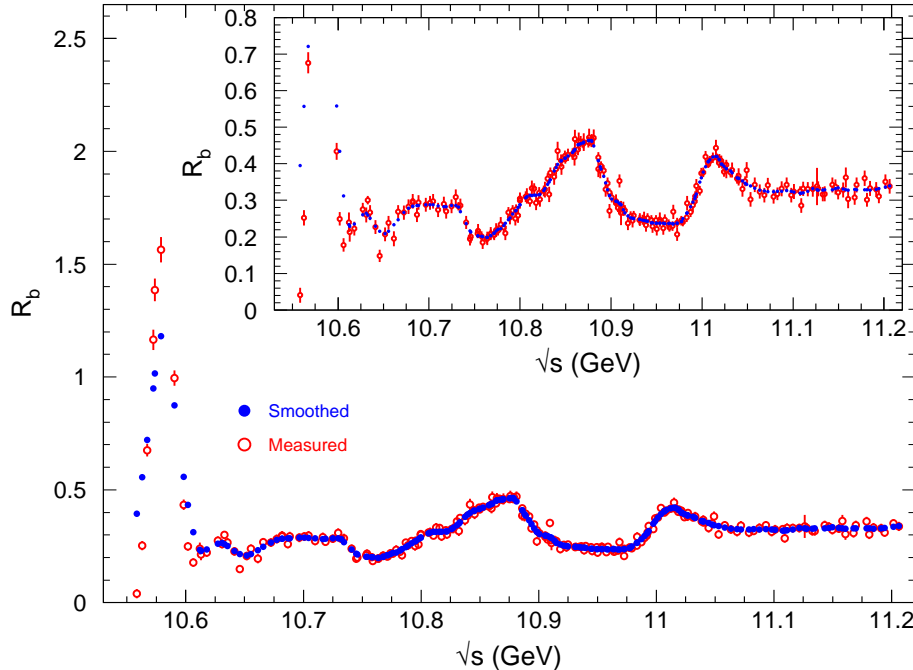


FIG. 5: Belle and BaBar combined R_b data (red circles with error bars) and the results after smoothing (blue dots). Error bars are combined statistical and systematic errors.

In the following analysis, we use a straight line to connect two neighboring points. As these points are after smoothing and the step is not big, there is no big jump between neighboring points, so we do not expect significant difference between a straight line and a smooth curve.

IV. CALCULATION PROCEDURE

A. Calculation of ISR correction factors

We follow the procedure defined in Eqs. (7), (8), and (9) to calculate the ISR correction factors. In doing this for experimental data, we assumed the detection efficiencies for $b\bar{b}$ events without ISR and those with different energy of ISR photons have been estimated reliably within the quoted systematic uncertainties at both BaBar [5] and Belle experiment [6]. The iteration is continued until the difference between two consecutive results is less than 1% of the statistical error of the observed R_b .

In the energy region where the cross section varies smoothly, the ISR correction factors become stable after a few iterations while in the $\Upsilon(4S)$ energy region, due to the rapid change of the cross section in narrow energy region, the ISR correction factors only converge to within 1% after more than ten iterations. We iterate 20 times, and the maximum difference is less than 0.5% within the full energy region. Figure 6 shows the final ISR factors as well as the corrected R_b^{dre} values.

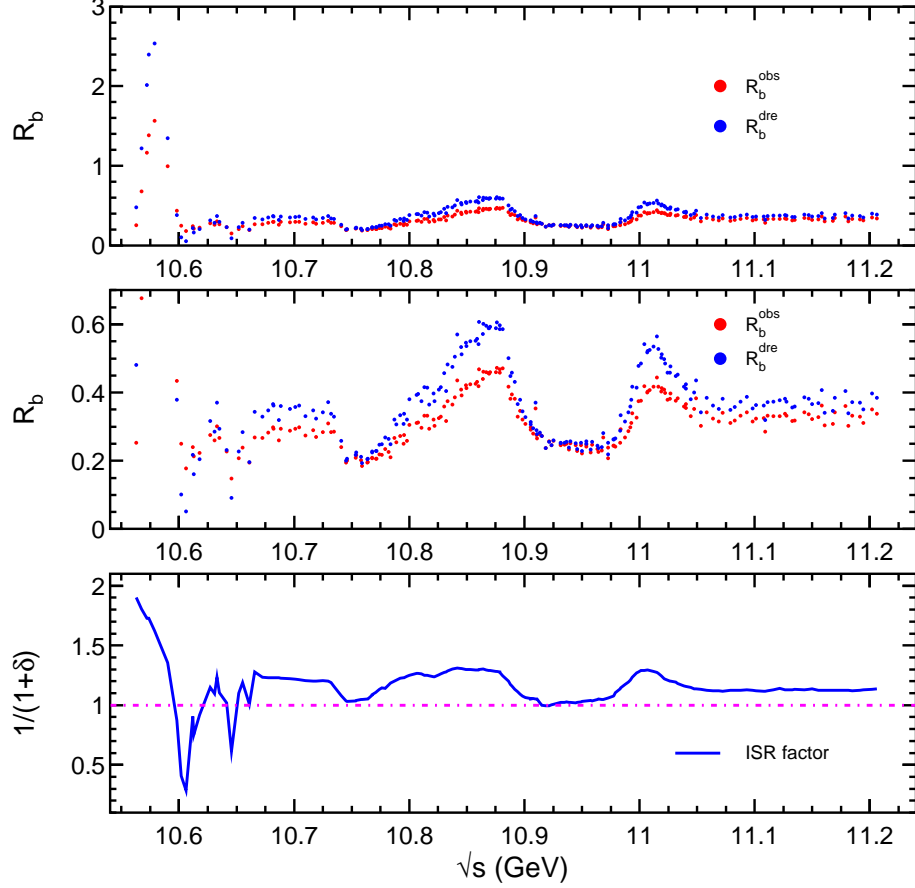


FIG. 6: Normalized R_b (red in the top two panels) and the ISR corrected R_b (or R_b^{dre} , blue in the top two panels), errors are not shown. The bottom panel shows the ISR correction factor.

B. Calculation of vacuum polarization factors

Taking R_b^{dre} , the ISR corrected R_b obtained in previous subsection, as the approximation of R_b^{B} and adding the pQCD calculation of the $udsc$ -quark contribution to R values (refer to Eq. (23)), we calculate the VP factors in the bottomonium energy region. After obtaining the VP factor $\frac{1}{|1-\Pi|^2}$, we use $R_b^{\text{dre}}/\frac{1}{|1-\Pi|^2}$ as input to calculate $\frac{1}{|1-\Pi|^2}$ again and we iterate this process. It turns out that after three iterations, the VP factor $\frac{1}{|1-\Pi|^2}$ becomes stable so we take the values from this round as the final results, and we obtain R_b^{B} with Eq. (20). Figure 7 shows the VP factors from this calculation.

C. Estimation of errors

In the previous two subsections we obtain the ISR correction factor and VP factor and in turn the Born R_b^{B} via Eq. (20). During the calculation, however, only the central values of the observed R_b are used. Instead of just scaling the errors of the original measurements by the obtained ISR correction factors and the VP factors, we perform a toy Monte Carlo sampling to investigate how the errors (both statistical and systematic) of the original measurements impact the obtained R_b^{B} .

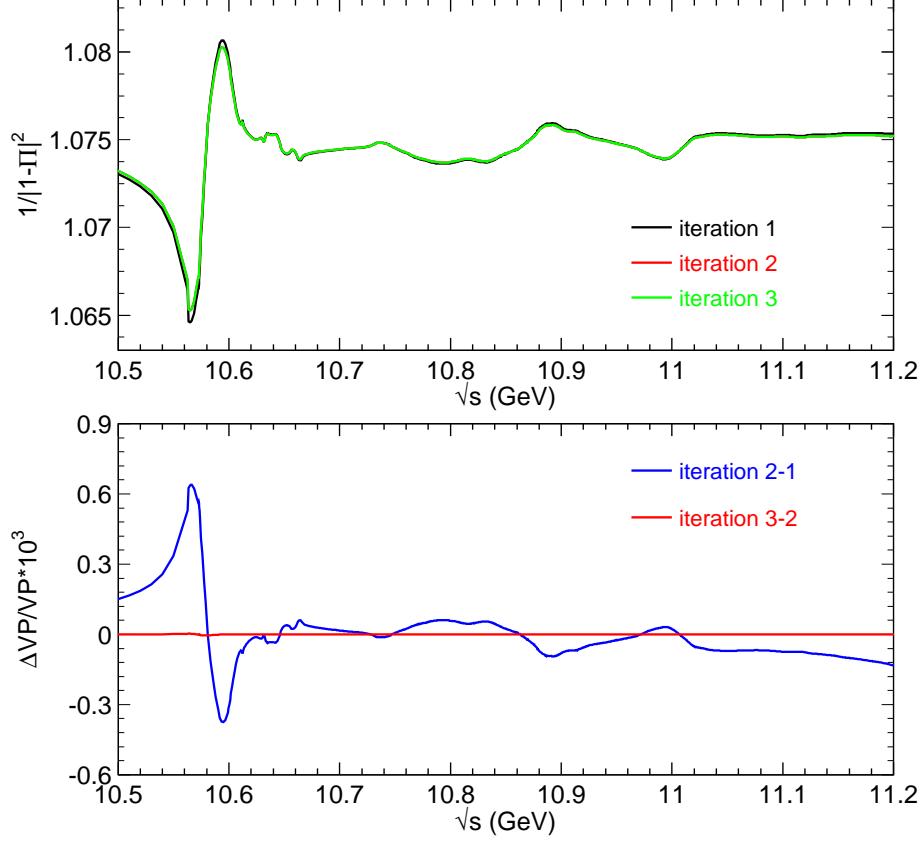


FIG. 7: The VP factors from 3 iterations (top) and the difference between two iterations (bottom). Notice that the difference between the second and the third iterations is very small and the curves for the VP factors are almost indistinguishable.

At each energy point where the Belle or BaBar measurement [5, 6] was performed, we perform 10,000 samplings of the observed R_b according to a Gaussian distribution for which the mean value and standard deviation are the central value and statistical error of the observed R_b , respectively. These samples will be used to estimate the statistical errors of the deduced quantities. In addition, the uncommon systematic errors are also added to the samples in the same way. For the common systematic error, the same error is added to each sample at all energy points in Belle or BaBar experiment. These samples with both statistical and systematic errors considered will yield the total errors of the deduced quantities. In the energy regions $0.36 < \sqrt{s} < 2.0$ GeV and $3.7 < \sqrt{s} < 5.0$ GeV, the data from the PDG compilation [1, 16] and BES collaboration [17, 18] are assumed to be completely correlated when we perform the sampling.

With each sample as input, we repeat the calculation described in the previous two subsections to obtain the ISR correction factor, VP factor, and R_b^B for this sample. Finally a distribution of R_b^B at each energy point is observed, so are the ISR correction factor and the VP factor. We find that these distributions also satisfy Gaussian distribution well so the fitted mean and standard deviation are taken as the central value and error of the corresponding quantities, respectively. The covariances of the distributions of Born and dressed cross sections at different energy points are also available in the supplemental material [23]. These covariances are useful in calculations where R_b^B or R_b^{dre} are inputs such as extracting the resonant parameters of the $Y(10750)$, $\Upsilon(5S)$, and $\Upsilon(6S)$ by fitting R_b^{dre} .

dressed cross sections are the right ones to be used to determine the resonant parameters of the vector bottomonium states. Together with the R values measured at other energy points and the R values calculated with pQCD, we calculate the VP factors. By applying VP correction, we obtain the Born cross section of $e^+e^- \rightarrow b\bar{b}$ from threshold to 11.21 GeV. These cross sections can be used for all the calculations related to the photon propagator, such as a_μ , the μ anomalous magnetic moment, and $\alpha(s)$, the running coupling constant of QED [2, 3].

In the following parts of this section, we discuss the usage of the data obtained in this study.

A. Vacuum polarization

The VP factors have been calculated by many groups [14, 25–28], with the experimental data and various theoretical inputs when the data are not available or less precise. Different techniques on how to handle the discrete data points and how to correct possible bias in data were developed. All these different treatments yield very similar results on hadronic contribution to a_μ and on the running of the α at $M_{Z^0}^2$, which indicates that the methods are all essentially applicable with current precision of data.

Previous calculations of the VP factors in the bottomonium energy region used either the resonant parameters of the $\Upsilon(4S)$, $\Upsilon(5S)$, and $\Upsilon(6S)$ reported by previous experiments [7, 8] which are very crude [26, 27] or the experimental data from previous experiments [7, 8] which gave the observed cross sections [28]. We recalculate the VP factors by using R_b^B obtained in this analysis based on high precision data from BaBar and Belle experiments [5, 6], with the ISR correction and VP factors properly considered. Although these new data have little effect on the VP factors far from the bottomonium energy region, they do change the VP factors in the bottomonium energy region as is shown in Fig. 9. The difference between this and the previous calculations [26, 27] is visible at some energies although all the calculations agree within errors.

B. Bottomonium spectroscopy

There are very clear structures in R_b^B distribution shown in Fig. 8. From low to high energy, we identify the $\Upsilon(4S)$ at 10.58 GeV, dips due to $B\bar{B}^* + c.c.$ and $B^*\bar{B}^*$ thresholds at 10.61 and 10.65 GeV, respectively, a dip at 10.75 GeV that may correspond to the $Y(10750)$ [29], and the $\Upsilon(5S)$ and $\Upsilon(6S)$ at 10.89 and 11.02 GeV, respectively.

The observed R_b values were used to extract the resonant parameters of the $\Upsilon(5S)$ and $\Upsilon(6S)$ in the BaBar [5] and Belle [6] publications. As the ISR correction effect is significant and is energy dependent, this suggests that the fit results are not reliable. To avoid the dip at around 10.75 GeV, both BaBar and Belle fitted data above 10.80 GeV only. A recent study of $e^+e^- \rightarrow \pi^+\pi^-\Upsilon$ revealed a new state, the $Y(10750)$, with a mass of $(10752.7 \pm 5.9^{+0.7}_{-1.1})$ MeV/ c^2 and width $(35.5^{+17.6+3.9}_{-11.3-3.3})$ MeV [29], at exactly the position of the dip in R_b^B . This indicates that the dip is very likely to be produced by the interference between a Breit-Wigner function and a smooth background component.

We do a least-square fit to the dressed $e^+e^- \rightarrow b\bar{b}$ cross sections ($\sigma^{\text{dre}} = \frac{\sigma^B}{|1-\Pi|^2}$) above 10.68 GeV with the coherent sum of a continuum amplitude (proportional to $1/\sqrt{s}$) and three Breit-Wigner functions with constant widths representing the structures at 10.75, 10.89, and

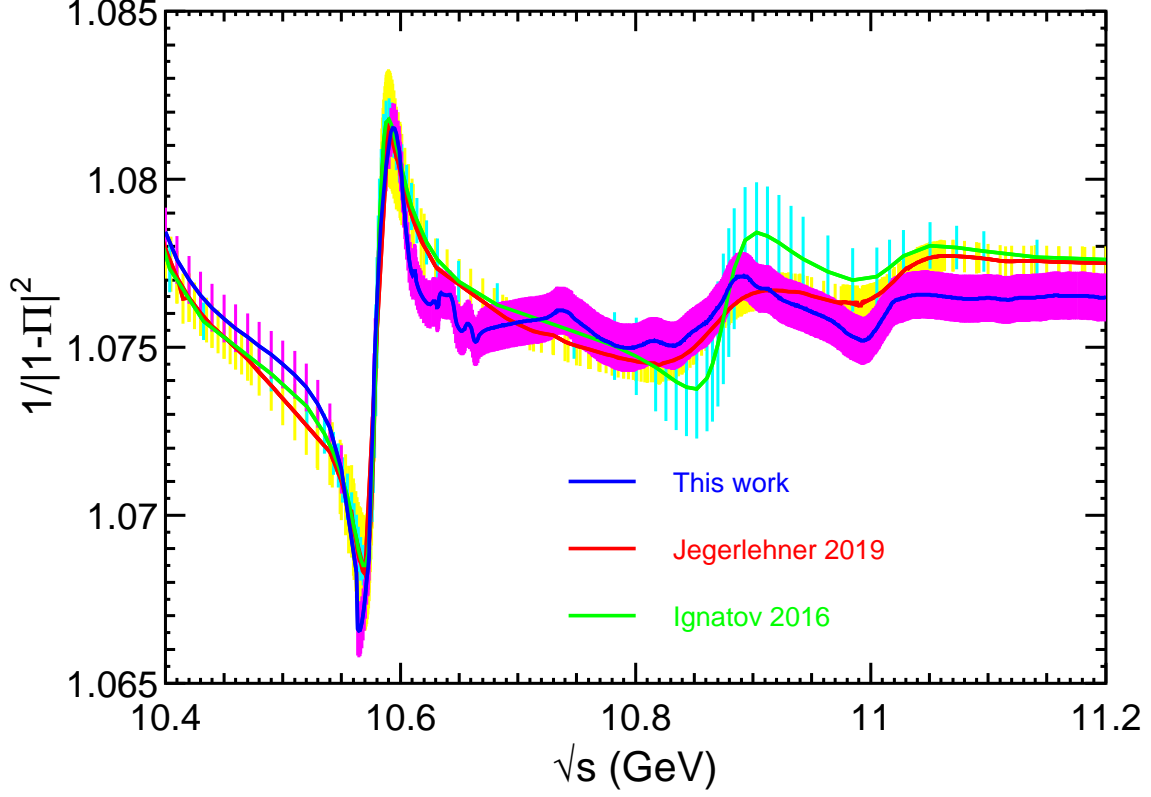


FIG. 9: VP factors in the bottomonium energy region and the comparison with previous calculations [26, 27]. The solid lines are the central values and the error bars or bands show the uncertainties.

11.02 GeV. The Breit-Wigner function is

$$\text{BW} = e^{i\phi} \frac{\sqrt{12\pi\Gamma_{e^+e^-}\Gamma}}{s - m^2 + im\Gamma},$$

where m , Γ , $\Gamma_{e^+e^-}$, and ϕ are the mass, total width, electronic partial width of the resonance, and the relative phase between the resonance and the real continuum amplitude, respectively, and they are all free parameters in the fits.

Eight sets of solutions are found from the fit [30], with identical total fit curve, identical fit quality ($\chi^2 = 274$ with 188 data points and 13 free parameters), and identical masses and widths for the same resonance, but with significantly different $\Gamma_{e^+e^-}$ and ϕ .

Figure 10 shows one of the solutions of the fit, and Table I lists the resonant parameters from 8 solutions of the fit. The masses and widths of the resonances agree with those from Ref. [29] but with improved precision because of the much better measurements used in this work compared with those in exclusive $e^+e^- \rightarrow \pi^+\pi^-\Upsilon$ analyses. The $\Gamma_{e^+e^-}$ values determined from this study allow us to extract the branching fractions of $\pi^+\pi^-\Upsilon$ of these resonances by combining the information reported in Ref. [29], and to understand the nature of these vector states [31–35].

In this analysis, we assumed that all the resonances are Breit-Wigner functions with constant widths and the continuum term is a smooth curve in the full energy region and they interfere with each other completely. In fact, the R_b^B or the total cross section has contributions from different modes, including open bottom and hidden bottom final states, the parametrization of the line shape should be very complicated due to the coupled-channel effect [36] and the presence

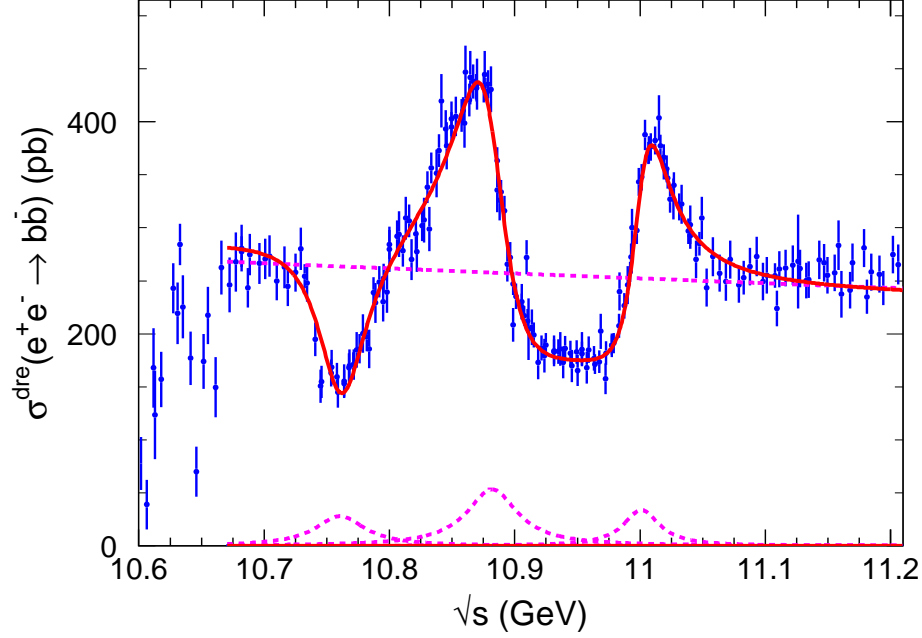


FIG. 10: Fit to the dressed cross sections with coherent sum of a continuum amplitude and three Breit-Wigner functions. The solid curve is the total fit, and the dashed ones for each of the four components from Sol. 1 in Table I. The magnitudes of these components are different in different solutions.

TABLE I: Resonant parameters from the fit to dressed cross sections. There are 8 solutions with identical fit quality, and the masses and widths of the resonances are identical in all the solutions. The uncertainties are combined statistical and systematic uncertainties in experimental measurements.

Solution	Parameter	$Y(10750)$	$\Upsilon(5S)$	$\Upsilon(6S)$
1–8	Mass (MeV/ c^2)	10761 ± 2	10882 ± 1	11001 ± 1
	Width (MeV)	48.5 ± 3.0	49.5 ± 1.5	35.1 ± 1.2
1	$\Gamma_{e^+e^-}$ (eV)	10.7 ± 0.9	21.3 ± 1.0	9.8 ± 0.5
	ϕ (degree)	260 ± 3	144 ± 2	34 ± 3
2	$\Gamma_{e^+e^-}$ (eV)	11.1 ± 0.9	24.8 ± 1.3	307 ± 9
	ϕ (degree)	270 ± 3	164 ± 2	280 ± 1
3	$\Gamma_{e^+e^-}$ (eV)	12.6 ± 1.1	479 ± 14	11.5 ± 0.6
	ϕ (degree)	295 ± 3	254 ± 1	3 ± 3
4	$\Gamma_{e^+e^-}$ (eV)	13.0 ± 1.1	558 ± 19	363 ± 13
	ϕ (degree)	296 ± 3	274 ± 1	249 ± 1
5	$\Gamma_{e^+e^-}$ (eV)	324 ± 24	23.7 ± 1.2	10.0 ± 0.5
	ϕ (degree)	265 ± 1	129 ± 2	26 ± 3
6	$\Gamma_{e^+e^-}$ (eV)	336 ± 27	27.6 ± 1.6	314 ± 10
	ϕ (degree)	275 ± 1	149 ± 2	272 ± 1
7	$\Gamma_{e^+e^-}$ (eV)	380 ± 32	534 ± 18	11.8 ± 0.6
	ϕ (degree)	291 ± 1	239 ± 1	355 ± 3
8	$\Gamma_{e^+e^-}$ (eV)	394 ± 34	622 ± 25	370 ± 14
	ϕ (degree)	301 ± 1	259 ± 2	241 ± 1

of many open bottom thresholds, $B\bar{B}$, $B\bar{B}^* + c.c.$, $B^*\bar{B}^*$, $B_s\bar{B}_s$, $B_s\bar{B}_s^* + c.c.$, $B_s^*\bar{B}_s^*$, $B\bar{B}_1 + c.c.$, $B^*\bar{B}_0 + c.c.$, $B^*\bar{B}_1 + c.c.$, $B\bar{B}_2 + c.c.$, and so on, and even $\pi Z_b(10610)$, $\pi Z_b(10650)$. The situation becomes somewhat simpler in a single final state like $\pi^+\pi^-\Upsilon(nS)$ ($n = 1, 2, 3$) [6] and $\pi^+\pi^-h_b(mP)$ ($m = 1, 2$) [37] although the intermediate structure in the three-body final state is also complicated. The results from these fits may change dramatically by including more information on each exclusive mode.

We also attempt to add one more Breit-Wigner function to fit the cross sections, the fit quality improves slightly with a state at $m = (10848 \pm 9) \text{ MeV}/c^2$ with a width of $(28 \pm 14) \text{ MeV}$, a state at $m = (10831 \pm 1) \text{ MeV}/c^2$ with a width of $(14 \pm 5) \text{ MeV}$, or a state at $m = (11065 \pm 23) \text{ MeV}/c^2$ with a width of $(73 \pm 37) \text{ MeV}$. In all these cases, the significance of the additional state is less than 4σ .

The data obtained in this analysis can be used to extract resonant parameters of these states if a better parametrization of the cross sections is developed.

C. Search for the production of invisible particles

The experimentally observed $e^+e^- \rightarrow \mu^+\mu^-$ cross section, with radiative correction is expressed as

$$\sigma(s)(e^+e^- \rightarrow \mu^+\mu^-) = \int_0^{x_m} \frac{4\pi\alpha^2}{3s(1-x)} \frac{F(x, s)}{|1 - \Pi(s(1-x))|^2} dx, \quad (24)$$

where $F(x, s)$ is expressed in Eq. (3), $x_m = 1 - s_m/s$, with $\sqrt{s_m}$ the required minimum invariant mass of the μ pair in the event selection. Here the mass of μ is neglected for charm and beauty factories. In Eq. (24), the cross section is calculated by QED without any ambiguity except the vacuum polarization $\Pi(s)$ which is expressed by Eqs. (10–15), with the hadronic contribution depending on the experimental measured data as input.

If the $e^+e^- \rightarrow \mu^+\mu^-$ cross section is measured to a high precision, then $\Pi(s)$ can be obtained. Thus $\Pi(s)$ is measured from the experiment directly [38]. It can then be compared with that calculated by Eqs. (10–15). This provides a test of QED at high luminosity flavor factories. In Eq. (10), the leptonic term $\Pi_l(s, m^2)$ is expressed in terms of the QED fine structure constant $\alpha(0)$ and lepton masses, which are all known to very high accuracy, while the hadronic term $\Pi_h(s)$ must be evaluated with Eq. (15) with the input of experimental measured hadronic cross sections. It is seen in Eq. (15) that $\Pi_h(s)$ is most sensitive to the hadronic cross section at energies close to s , which can be measured with the same experiment. Therefore such a test of QED can be performed with two sets of data, $e^+e^- \rightarrow \mu^+\mu^-$ and $e^+e^- \rightarrow \text{hadrons}$, collected within the same experiment. Any discrepancy would mean that there are missing hadronic final states, or even a final state that escaped detection, or is invisible by current detection technology. This provides a test of QED and search for new physics. We propose for it to be included in physics goals in future high-luminosity frontier physics.

Acknowledgments

This work is supported in part by National Natural Science Foundation of China (NSFC) under contract Nos. 11521505, 11475187, and 11375206; Key Research Program of Frontier Sciences, CAS, Grant No. QYZDJ-SSW-SLH011; the CAS Center for Excellence in Particle Physics

(CCEPP); and the Munich Institute for Astro- and Particle Physics (MIAPP) which is funded by the Deutsche Forschungsgemeinschaft (DFG, German Research Foundation) under Germany's Excellence Strategy-EXC-2094-390783311.

-
- [1] V. V. Ezhela, S. B. Lugovsky and O. V. Zenin, hep-ph/0312114.
 - [2] M. Davier, A. Hoecker, B. Malaescu and Z. Zhang, Eur. Phys. J. C **80**, no. 3, 241 (2020).
 - [3] A. Keshavarzi, D. Nomura and T. Teubner, Phys. Rev. D **101**, no. 1, 014029 (2020).
 - [4] F. Jegerlehner, EPJ Web Conf. **166**, 00022 (2018).
 - [5] B. Aubert *et al.* [BaBar Collaboration], Phys. Rev. Lett. **102**, 012001 (2009).
 - [6] D. Santel *et al.* [Belle Collaboration], Phys. Rev. D **93**, no. 1, 011101 (2016).
 - [7] D. M. J. Lovelock *et al.*, Phys. Rev. Lett. **54**, 377 (1985).
 - [8] D. Besson *et al.* [CLEO Collaboration], Phys. Rev. Lett. **54**, 381 (1985).
 - [9] E. A. Kuraev and V. S. Fadin, Sov. J. Nucl. Phys. **41**, 466 (1985) [Yad. Fiz. **41**, 733 (1985).]
 - [10] F. A. Berends, “Z Line Shape”, CERN **89-08** (1989), edited by G. Altarelli, R. Kleiss and C. Verzegnassi.
 - [11] G. Montagna, O. Nicrosini, F. Piccinini and L. Trentadue, Nucl. Phys. B **452**, 161 (1995).
 - [12] X. K. Dong, L. L. Wang and C. Z. Yuan, Chin. Phys. C **42**, no. 4, 043002 (2018).
 - [13] W. Greiner, J. Reinhardt. Quantum Electrodynamics (3rd Ed.), Springer-Verlag, Berlin, 1994.
 - [14] F. A. Berends and G. J. Komen, Phys. Lett. **63B**, 432 (1976).
 - [15] M. Davier, S. Eidelman, A. Hocker and Z. Zhang, Eur. Phys. J. C **27**, 497 (2003).
 - [16] M. Tanabashi *et al.* [Particle Data Group], Phys. Rev. D **98**, no. 3, 030001 (2018).
 - [17] J. Z. Bai *et al.* [BES Collaboration], Phys. Rev. Lett. **84**, 594 (2000).
 - [18] J. Z. Bai *et al.* [BES Collaboration], Phys. Rev. Lett. **88**, 101802 (2002).
 - [19] G. Rodrigo, A. Pich and A. Santamaria, Phys. Lett. B **424**, 367 (1998).
 - [20] V. V. Anashin *et al.* [KEDR Collaboration], Phys. Lett. B **788**, 42 (2019).
 - [21] V. V. Anashin *et al.*, Phys. Lett. B **770**, 174 (2017).
 - [22] William S. Cleveland (Wadsworth, 555 Morego Street, Monterey, California 93940), “The Elements of Graphing Data”. We use the program from wikipedia (https://en.wikipedia.org/wiki/Local_regression) supplied by the author.
 - [23] See supplemental material at <http://cpc.ihep.ac.cn/article/doi/10.1088/1674-1137/44/8/083001> for the final results shown in the Appendix and the covariances of the R_b^B and R_b^{dre} .
 - [24] <https://www.mathworks.com/help/curvefit/smoothing-splines.html>
 - [25] S. Actis *et al.* [Working Group on Radiative Corrections and Monte Carlo Generators for Low Energies], Eur. Phys. J. C **66**, 585 (2010) and references therein.
 - [26] Fred Jegerlehner, <http://www-com.physik.hu-berlin.de/~fjeger/software.html> and the references therein.
 - [27] Fedor Ignatov, talk at the fourth meeting of the Working Group on Rad. Corrections and MC Generators for Low Energies, Beijing, October 9-11, 2008. http://www.lnf.infn.it/wg/sighad/beijing08/Sighadmeeting/sighad08_vpol.pdf.
 - [28] K. Hagiwara, A. D. Martin, D. Nomura and T. Teubner, Phys. Rev. D **69**, 093003 (2004); K. Hagiwara, A. D. Martin, D. Nomura and T. Teubner, Phys. Lett. B **649**, 173 (2007).
 - [29] R. Mizuk *et al.* [Belle Collaboration], JHEP **1910**, 220 (2019).
 - [30] K. Zhu, X. H. Mo, C. Z. Yuan and P. Wang, Int. J. Mod. Phys. A **26**, 4511 (2011).
 - [31] See, for example, B. Chen, A. Zhang and J. He, Phys. Rev. D **101**, no. 1, 014020 (2020), and references

therein.

- [32] A. Ali, L. Maiani, A. Y. Parkhomenko and W. Wang, Phys. Lett. B **802**, 135217 (2020).
- [33] Q. Li, M. S. Liu, Q. F. L, L. C. Gui and X. H. Zhong, Eur. Phys. J. C **80**, no. 1, 59 (2020).
- [34] Z. G. Wang, Chin. Phys. C **43**, no. 12, 123102 (2019).
- [35] W. H. Liang, N. Ikeno and E. Oset, Phys. Lett. B **803**, 135340 (2020).
- [36] N. A. Tornqvist, Phys. Rev. Lett. **53**, 878 (1984).
- [37] A. Abdesselam *et al.* [Belle Collaboration], Phys. Rev. Lett. **117**, no. 14, 142001 (2016).
- [38] A. Anastasi *et al.* [KLOE-2 Collaboration], Phys. Lett. B **767**, 485 (2017).

Appendix A: Final results of Born cross section R_b^B and dressed cross section R_b^{dre} , together with the ISR correction factors and vacuum polarization factors. The first error of R_b^B and R_b^{dre} is statistical and the second one is systematic. The errors of ISR factor and VP factor are combined statistical and systematic errors.

\sqrt{s} (GeV)	R_b^B	R_b^{dre}	$1/(1 + \delta)$	$1/ 1 - \Pi ^2$
10.5628	$0.4498 \pm 0.0341 \pm 0.0155$	$0.4799 \pm 0.0364 \pm 0.0164$	1.9009 ± 0.0000	1.0670 ± 0.0008
10.5673	$1.1436 \pm 0.0399 \pm 0.0308$	$1.2199 \pm 0.0425 \pm 0.0325$	1.8044 ± 0.0074	1.0668 ± 0.0008
10.5723	$1.8835 \pm 0.0598 \pm 0.0487$	$2.0122 \pm 0.0642 \pm 0.0516$	1.7273 ± 0.0063	1.0683 ± 0.0008
10.5738	$2.2419 \pm 0.0714 \pm 0.0574$	$2.3981 \pm 0.0760 \pm 0.0610$	1.7294 ± 0.0126	1.0697 ± 0.0008
10.5788	$2.3593 \pm 0.0700 \pm 0.0598$	$2.5363 \pm 0.0750 \pm 0.0642$	1.6218 ± 0.0082	1.0750 ± 0.0008
10.5903	$1.2485 \pm 0.0372 \pm 0.0323$	$1.3496 \pm 0.0402 \pm 0.0350$	1.3543 ± 0.0121	1.0809 ± 0.0008
10.5983	$0.3508 \pm 0.0326 \pm 0.0119$	$0.3791 \pm 0.0353 \pm 0.0128$	0.8728 ± 0.0438	1.0809 ± 0.0008
10.6018	$0.0943 \pm 0.0289 \pm 0.0059$	$0.1019 \pm 0.0312 \pm 0.0063$	0.4002 ± 0.1016	1.0797 ± 0.0008
10.6063	$0.0465 \pm 0.0270 \pm 0.0053$	$0.0501 \pm 0.0291 \pm 0.0057$	0.2732 ± 0.1383	1.0779 ± 0.0008
10.6118	$0.2022 \pm 0.0444 \pm 0.0079$	$0.2178 \pm 0.0478 \pm 0.0085$	0.8942 ± 0.1092	1.0771 ± 0.0008
10.6128	$0.1488 \pm 0.0498 \pm 0.0083$	$0.1603 \pm 0.0536 \pm 0.0090$	0.7332 ± 0.1801	1.0771 ± 0.0008
10.6178	$0.1892 \pm 0.0301 \pm 0.0082$	$0.2037 \pm 0.0324 \pm 0.0089$	0.9110 ± 0.0810	1.0765 ± 0.0008
10.6273	$0.2938 \pm 0.0263 \pm 0.0102$	$0.3162 \pm 0.0283 \pm 0.0110$	1.1466 ± 0.0401	1.0763 ± 0.0008
10.6308	$0.2648 \pm 0.0331 \pm 0.0102$	$0.2850 \pm 0.0356 \pm 0.0110$	1.0919 ± 0.0638	1.0762 ± 0.0008
10.6328	$0.3440 \pm 0.0067 \pm 0.0228$	$0.3702 \pm 0.0072 \pm 0.0245$	1.2330 ± 0.0444	1.0763 ± 0.0008
10.6353	$0.2728 \pm 0.0335 \pm 0.0123$	$0.2937 \pm 0.0360 \pm 0.0133$	1.0989 ± 0.0658	1.0766 ± 0.0008
10.6413	$0.2145 \pm 0.0293 \pm 0.0082$	$0.2310 \pm 0.0315 \pm 0.0088$	1.0136 ± 0.0666	1.0765 ± 0.0008
10.6458	$0.0848 \pm 0.0287 \pm 0.0048$	$0.0912 \pm 0.0308 \pm 0.0051$	0.6015 ± 0.1485	1.0761 ± 0.0008
10.6518	$0.2120 \pm 0.0297 \pm 0.0103$	$0.2279 \pm 0.0319 \pm 0.0111$	1.0931 ± 0.0681	1.0754 ± 0.0008
10.6553	$0.2637 \pm 0.0312 \pm 0.0103$	$0.2836 \pm 0.0335 \pm 0.0111$	1.1868 ± 0.0602	1.0755 ± 0.0008
10.6613	$0.1820 \pm 0.0335 \pm 0.0086$	$0.1957 \pm 0.0360 \pm 0.0093$	0.9961 ± 0.0892	1.0755 ± 0.0008
10.6659	$0.3194 \pm 0.0255 \pm 0.0116$	$0.3434 \pm 0.0275 \pm 0.0125$	1.2768 ± 0.0358	1.0754 ± 0.0008
10.6724	$0.3059 \pm 0.0207 \pm 0.0105$	$0.3290 \pm 0.0223 \pm 0.0113$	1.2326 ± 0.0118	1.0754 ± 0.0008
10.6774	$0.3236 \pm 0.0218 \pm 0.0102$	$0.3480 \pm 0.0235 \pm 0.0110$	1.2307 ± 0.0104	1.0755 ± 0.0008
10.6819	$0.3405 \pm 0.0225 \pm 0.0101$	$0.3662 \pm 0.0241 \pm 0.0109$	1.2306 ± 0.0128	1.0755 ± 0.0008
10.6820	$0.3364 \pm 0.0040 \pm 0.0148$	$0.3618 \pm 0.0043 \pm 0.0159$	1.2306 ± 0.0128	1.0755 ± 0.0008
10.6869	$0.2975 \pm 0.0209 \pm 0.0103$	$0.3200 \pm 0.0225 \pm 0.0110$	1.2273 ± 0.0130	1.0756 ± 0.0008
10.6884	$0.3357 \pm 0.0230 \pm 0.0104$	$0.3611 \pm 0.0247 \pm 0.0112$	1.2244 ± 0.0138	1.0756 ± 0.0008
10.6964	$0.3273 \pm 0.0206 \pm 0.0108$	$0.3521 \pm 0.0221 \pm 0.0116$	1.2215 ± 0.0122	1.0757 ± 0.0008
10.7009	$0.3321 \pm 0.0213 \pm 0.0108$	$0.3573 \pm 0.0229 \pm 0.0116$	1.2181 ± 0.0129	1.0757 ± 0.0008
10.7044	$0.3357 \pm 0.0221 \pm 0.0107$	$0.3611 \pm 0.0237 \pm 0.0115$	1.2138 ± 0.0114	1.0757 ± 0.0008
10.7099	$0.3073 \pm 0.0204 \pm 0.0102$	$0.3305 \pm 0.0219 \pm 0.0110$	1.2059 ± 0.0113	1.0758 ± 0.0008
10.7164	$0.3233 \pm 0.0224 \pm 0.0102$	$0.3478 \pm 0.0241 \pm 0.0110$	1.1990 ± 0.0134	1.0758 ± 0.0008
10.7189	$0.3016 \pm 0.0207 \pm 0.0100$	$0.3245 \pm 0.0223 \pm 0.0108$	1.2010 ± 0.0123	1.0758 ± 0.0008
10.7249	$0.3177 \pm 0.0204 \pm 0.0096$	$0.3418 \pm 0.0219 \pm 0.0103$	1.2050 ± 0.0106	1.0759 ± 0.0008
10.7294	$0.3455 \pm 0.0222 \pm 0.0105$	$0.3718 \pm 0.0239 \pm 0.0113$	1.2029 ± 0.0129	1.0759 ± 0.0008
10.7322	$0.3137 \pm 0.0039 \pm 0.0136$	$0.3375 \pm 0.0042 \pm 0.0147$	1.1886 ± 0.0132	1.0760 ± 0.0008
10.7344	$0.3062 \pm 0.0197 \pm 0.0092$	$0.3295 \pm 0.0212 \pm 0.0099$	1.1527 ± 0.0119	1.0761 ± 0.0008
10.7409	$0.2411 \pm 0.0183 \pm 0.0076$	$0.2594 \pm 0.0196 \pm 0.0082$	1.0802 ± 0.0181	1.0760 ± 0.0008

\sqrt{s} (GeV)	R_b^B	R_b^{dre}	$1/(1 + \delta)$	$1/ 1 - \Pi ^2$
10.7449	$0.1868 \pm 0.0179 \pm 0.0067$	$0.2010 \pm 0.0192 \pm 0.0072$	1.0337 ± 0.0225	1.0760 ± 0.0008
10.7459	$0.1917 \pm 0.0178 \pm 0.0065$	$0.2062 \pm 0.0191 \pm 0.0070$	1.0271 ± 0.0226	1.0759 ± 0.0008
10.7535	$0.2016 \pm 0.0077 \pm 0.0140$	$0.2169 \pm 0.0082 \pm 0.0151$	1.0363 ± 0.0240	1.0757 ± 0.0008
10.7539	$0.2088 \pm 0.0192 \pm 0.0069$	$0.2246 \pm 0.0207 \pm 0.0074$	1.0372 ± 0.0232	1.0757 ± 0.0008
10.7579	$0.1973 \pm 0.0081 \pm 0.0145$	$0.2122 \pm 0.0087 \pm 0.0156$	1.0485 ± 0.0255	1.0756 ± 0.0008
10.7589	$0.1800 \pm 0.0172 \pm 0.0059$	$0.1935 \pm 0.0185 \pm 0.0063$	1.0482 ± 0.0234	1.0755 ± 0.0008
10.7637	$0.1901 \pm 0.0081 \pm 0.0137$	$0.2045 \pm 0.0087 \pm 0.0147$	1.0507 ± 0.0241	1.0754 ± 0.0008
10.7639	$0.1926 \pm 0.0188 \pm 0.0059$	$0.2071 \pm 0.0202 \pm 0.0064$	1.0535 ± 0.0236	1.0754 ± 0.0008
10.7677	$0.2089 \pm 0.0081 \pm 0.0147$	$0.2247 \pm 0.0087 \pm 0.0158$	1.0848 ± 0.0238	1.0753 ± 0.0008
10.7679	$0.2113 \pm 0.0180 \pm 0.0070$	$0.2272 \pm 0.0194 \pm 0.0075$	1.0865 ± 0.0231	1.0753 ± 0.0008
10.7711	$0.2121 \pm 0.0037 \pm 0.0148$	$0.2280 \pm 0.0039 \pm 0.0159$	1.1097 ± 0.0240	1.0752 ± 0.0008
10.7716	$0.2129 \pm 0.0084 \pm 0.0157$	$0.2289 \pm 0.0091 \pm 0.0169$	1.1118 ± 0.0238	1.0752 ± 0.0008
10.7739	$0.2302 \pm 0.0198 \pm 0.0074$	$0.2475 \pm 0.0213 \pm 0.0080$	1.1309 ± 0.0199	1.0752 ± 0.0008
10.7760	$0.2315 \pm 0.0092 \pm 0.0146$	$0.2489 \pm 0.0099 \pm 0.0157$	1.1437 ± 0.0214	1.0751 ± 0.0008
10.7789	$0.2491 \pm 0.0202 \pm 0.0098$	$0.2679 \pm 0.0217 \pm 0.0106$	1.1415 ± 0.0175	1.0751 ± 0.0008
10.7820	$0.2452 \pm 0.0086 \pm 0.0146$	$0.2636 \pm 0.0092 \pm 0.0157$	1.1684 ± 0.0159	1.0750 ± 0.0008
10.7839	$0.2310 \pm 0.0204 \pm 0.0094$	$0.2483 \pm 0.0219 \pm 0.0101$	1.1831 ± 0.0150	1.0750 ± 0.0008
10.7871	$0.2979 \pm 0.0087 \pm 0.0160$	$0.3202 \pm 0.0093 \pm 0.0172$	1.1999 ± 0.0144	1.0750 ± 0.0008
10.7889	$0.2861 \pm 0.0209 \pm 0.0111$	$0.3076 \pm 0.0225 \pm 0.0119$	1.2116 ± 0.0139	1.0750 ± 0.0008
10.7920	$0.3106 \pm 0.0089 \pm 0.0157$	$0.3339 \pm 0.0096 \pm 0.0169$	1.2251 ± 0.0130	1.0750 ± 0.0008
10.7949	$0.2869 \pm 0.0213 \pm 0.0102$	$0.3084 \pm 0.0229 \pm 0.0109$	1.2296 ± 0.0127	1.0750 ± 0.0008
10.7955	$0.3145 \pm 0.0083 \pm 0.0153$	$0.3381 \pm 0.0089 \pm 0.0164$	1.2311 ± 0.0130	1.0750 ± 0.0008
10.7979	$0.2978 \pm 0.0218 \pm 0.0112$	$0.3201 \pm 0.0234 \pm 0.0120$	1.2407 ± 0.0132	1.0750 ± 0.0008
10.7999	$0.3540 \pm 0.0082 \pm 0.0156$	$0.3805 \pm 0.0088 \pm 0.0167$	1.2498 ± 0.0106	1.0750 ± 0.0008
10.8063	$0.3655 \pm 0.0096 \pm 0.0164$	$0.3930 \pm 0.0104 \pm 0.0176$	1.2668 ± 0.0111	1.0750 ± 0.0008
10.8075	$0.3675 \pm 0.0234 \pm 0.0126$	$0.3951 \pm 0.0251 \pm 0.0135$	1.2665 ± 0.0102	1.0751 ± 0.0008
10.8107	$0.3486 \pm 0.0093 \pm 0.0155$	$0.3748 \pm 0.0100 \pm 0.0166$	1.2616 ± 0.0096	1.0751 ± 0.0008
10.8130	$0.3876 \pm 0.0222 \pm 0.0127$	$0.4167 \pm 0.0238 \pm 0.0136$	1.2522 ± 0.0082	1.0751 ± 0.0008
10.8157	$0.3846 \pm 0.0098 \pm 0.0167$	$0.4136 \pm 0.0105 \pm 0.0180$	1.2478 ± 0.0108	1.0752 ± 0.0008
10.8175	$0.3389 \pm 0.0215 \pm 0.0109$	$0.3644 \pm 0.0231 \pm 0.0118$	1.2436 ± 0.0106	1.0752 ± 0.0008
10.8210	$0.3694 \pm 0.0094 \pm 0.0167$	$0.3972 \pm 0.0101 \pm 0.0180$	1.2387 ± 0.0102	1.0751 ± 0.0008
10.8220	$0.3487 \pm 0.0216 \pm 0.0120$	$0.3749 \pm 0.0232 \pm 0.0129$	1.2387 ± 0.0105	1.0751 ± 0.0008
10.8259	$0.3796 \pm 0.0094 \pm 0.0160$	$0.4081 \pm 0.0101 \pm 0.0172$	1.2536 ± 0.0096	1.0751 ± 0.0008
10.8275	$0.3862 \pm 0.0230 \pm 0.0142$	$0.4152 \pm 0.0248 \pm 0.0153$	1.2607 ± 0.0094	1.0750 ± 0.0008
10.8304	$0.4252 \pm 0.0090 \pm 0.0167$	$0.4571 \pm 0.0097 \pm 0.0180$	1.2721 ± 0.0102	1.0750 ± 0.0008
10.8320	$0.3762 \pm 0.0215 \pm 0.0147$	$0.4044 \pm 0.0231 \pm 0.0158$	1.2773 ± 0.0090	1.0750 ± 0.0008
10.8332	$0.4486 \pm 0.0090 \pm 0.0161$	$0.4823 \pm 0.0097 \pm 0.0173$	1.2859 ± 0.0078	1.0750 ± 0.0008
10.8375	$0.4426 \pm 0.0235 \pm 0.0161$	$0.4759 \pm 0.0252 \pm 0.0174$	1.3047 ± 0.0088	1.0751 ± 0.0008
10.8396	$0.4691 \pm 0.0102 \pm 0.0167$	$0.5044 \pm 0.0109 \pm 0.0179$	1.3079 ± 0.0087	1.0751 ± 0.0008
10.8415	$0.5296 \pm 0.0251 \pm 0.0203$	$0.5695 \pm 0.0270 \pm 0.0218$	1.3094 ± 0.0085	1.0752 ± 0.0008
10.8450	$0.4959 \pm 0.0097 \pm 0.0198$	$0.5332 \pm 0.0104 \pm 0.0212$	1.3056 ± 0.0074	1.0753 ± 0.0008
10.8455	$0.4758 \pm 0.0232 \pm 0.0159$	$0.5117 \pm 0.0250 \pm 0.0171$	1.3049 ± 0.0076	1.0753 ± 0.0008
10.8494	$0.5080 \pm 0.0093 \pm 0.0184$	$0.5464 \pm 0.0100 \pm 0.0198$	1.2981 ± 0.0114	1.0755 ± 0.0008
10.8497	$0.4978 \pm 0.0030 \pm 0.0180$	$0.5353 \pm 0.0032 \pm 0.0194$	1.2978 ± 0.0109	1.0755 ± 0.0008

\sqrt{s} (GeV)	R_b^B	R_b^{dre}	$1/(1 + \delta)$	$1/ 1 - \Pi ^2$
10.8528	$0.5113 \pm 0.0099 \pm 0.0210$	$0.5499 \pm 0.0106 \pm 0.0226$	1.2968 ± 0.0121	1.0755 ± 0.0008
10.8577	$0.5126 \pm 0.0099 \pm 0.0173$	$0.5514 \pm 0.0106 \pm 0.0186$	1.2940 ± 0.0075	1.0757 ± 0.0008
10.8589	$0.5186 \pm 0.0035 \pm 0.0157$	$0.5579 \pm 0.0037 \pm 0.0168$	1.2955 ± 0.0074	1.0757 ± 0.0008
10.8600	$0.5043 \pm 0.0232 \pm 0.0176$	$0.5425 \pm 0.0250 \pm 0.0189$	1.2960 ± 0.0077	1.0757 ± 0.0008
10.8605	$0.5648 \pm 0.0248 \pm 0.0195$	$0.6076 \pm 0.0266 \pm 0.0209$	1.2966 ± 0.0080	1.0757 ± 0.0008
10.8639	$0.5314 \pm 0.0107 \pm 0.0167$	$0.5718 \pm 0.0115 \pm 0.0180$	1.3026 ± 0.0088	1.0759 ± 0.0008
10.8645	$0.5586 \pm 0.0263 \pm 0.0182$	$0.6010 \pm 0.0283 \pm 0.0196$	1.3018 ± 0.0097	1.0759 ± 0.0008
10.8667	$0.5538 \pm 0.0099 \pm 0.0177$	$0.5958 \pm 0.0106 \pm 0.0191$	1.2952 ± 0.0065	1.0760 ± 0.0008
10.8690	$0.5474 \pm 0.0033 \pm 0.0153$	$0.5890 \pm 0.0035 \pm 0.0164$	1.2914 ± 0.0076	1.0761 ± 0.0008
10.8695	$0.5462 \pm 0.0032 \pm 0.0162$	$0.5878 \pm 0.0034 \pm 0.0174$	1.2909 ± 0.0064	1.0761 ± 0.0008
10.8700	$0.5511 \pm 0.0249 \pm 0.0176$	$0.5931 \pm 0.0268 \pm 0.0190$	1.2902 ± 0.0069	1.0761 ± 0.0008
10.8752	$0.5472 \pm 0.0071 \pm 0.0165$	$0.5891 \pm 0.0076 \pm 0.0177$	1.2829 ± 0.0059	1.0764 ± 0.0008
10.8760	$0.5630 \pm 0.0230 \pm 0.0179$	$0.6060 \pm 0.0248 \pm 0.0192$	1.2822 ± 0.0057	1.0765 ± 0.0008
10.8785	$0.5436 \pm 0.0036 \pm 0.0157$	$0.5853 \pm 0.0039 \pm 0.0169$	1.2767 ± 0.0071	1.0767 ± 0.0008
10.8788	$0.5538 \pm 0.0062 \pm 0.0159$	$0.5962 \pm 0.0067 \pm 0.0171$	1.2748 ± 0.0073	1.0767 ± 0.0008
10.8810	$0.5442 \pm 0.0212 \pm 0.0163$	$0.5860 \pm 0.0228 \pm 0.0176$	1.2441 ± 0.0054	1.0768 ± 0.0008
10.8860	$0.4648 \pm 0.0086 \pm 0.0148$	$0.5006 \pm 0.0092 \pm 0.0160$	1.1993 ± 0.0073	1.0770 ± 0.0008
10.8880	$0.4162 \pm 0.0206 \pm 0.0127$	$0.4483 \pm 0.0222 \pm 0.0137$	1.1740 ± 0.0085	1.0771 ± 0.0008
10.8889	$0.4254 \pm 0.0034 \pm 0.0141$	$0.4582 \pm 0.0037 \pm 0.0152$	1.1625 ± 0.0084	1.0771 ± 0.0008
10.8918	$0.4009 \pm 0.0087 \pm 0.0150$	$0.4319 \pm 0.0094 \pm 0.0161$	1.1326 ± 0.0093	1.0771 ± 0.0008
10.8940	$0.3405 \pm 0.0179 \pm 0.0103$	$0.3667 \pm 0.0193 \pm 0.0111$	1.1132 ± 0.0103	1.0771 ± 0.0008
10.8962	$0.3514 \pm 0.0088 \pm 0.0174$	$0.3784 \pm 0.0095 \pm 0.0187$	1.0909 ± 0.0135	1.0770 ± 0.0008
10.8985	$0.3207 \pm 0.0029 \pm 0.0141$	$0.3453 \pm 0.0031 \pm 0.0152$	1.0754 ± 0.0120	1.0770 ± 0.0008
10.9009	$0.3038 \pm 0.0084 \pm 0.0139$	$0.3272 \pm 0.0090 \pm 0.0150$	1.0637 ± 0.0130	1.0769 ± 0.0008
10.9055	$0.2906 \pm 0.0184 \pm 0.0103$	$0.3129 \pm 0.0198 \pm 0.0111$	1.0526 ± 0.0124	1.0768 ± 0.0008
10.9056	$0.2850 \pm 0.0086 \pm 0.0122$	$0.3069 \pm 0.0093 \pm 0.0132$	1.0525 ± 0.0126	1.0768 ± 0.0008
10.9077	$0.2742 \pm 0.0041 \pm 0.0108$	$0.2952 \pm 0.0044 \pm 0.0116$	1.0572 ± 0.0149	1.0768 ± 0.0008
10.9095	$0.3449 \pm 0.0161 \pm 0.0128$	$0.3713 \pm 0.0173 \pm 0.0137$	1.0516 ± 0.0176	1.0768 ± 0.0008
10.9104	$0.2689 \pm 0.0087 \pm 0.0115$	$0.2896 \pm 0.0094 \pm 0.0124$	1.0502 ± 0.0191	1.0768 ± 0.0008
10.9110	$0.2589 \pm 0.0356 \pm 0.0101$	$0.2787 \pm 0.0383 \pm 0.0108$	1.0495 ± 0.0207	1.0768 ± 0.0008
10.9135	$0.2626 \pm 0.0193 \pm 0.0101$	$0.2827 \pm 0.0208 \pm 0.0108$	1.0178 ± 0.0198	1.0767 ± 0.0008
10.9152	$0.2526 \pm 0.0089 \pm 0.0120$	$0.2720 \pm 0.0096 \pm 0.0129$	0.9982 ± 0.0208	1.0767 ± 0.0008
10.9185	$0.2201 \pm 0.0185 \pm 0.0087$	$0.2370 \pm 0.0199 \pm 0.0094$	0.9954 ± 0.0172	1.0766 ± 0.0008
10.9215	$0.2373 \pm 0.0084 \pm 0.0126$	$0.2555 \pm 0.0091 \pm 0.0136$	0.9966 ± 0.0193	1.0765 ± 0.0008
10.9235	$0.2281 \pm 0.0182 \pm 0.0084$	$0.2455 \pm 0.0196 \pm 0.0091$	1.0018 ± 0.0159	1.0764 ± 0.0008
10.9250	$0.2410 \pm 0.0079 \pm 0.0124$	$0.2594 \pm 0.0085 \pm 0.0134$	1.0058 ± 0.0151	1.0764 ± 0.0008
10.9313	$0.2338 \pm 0.0081 \pm 0.0126$	$0.2517 \pm 0.0088 \pm 0.0136$	1.0224 ± 0.0164	1.0763 ± 0.0008
10.9315	$0.2345 \pm 0.0168 \pm 0.0086$	$0.2524 \pm 0.0181 \pm 0.0093$	1.0221 ± 0.0159	1.0763 ± 0.0008
10.9348	$0.2344 \pm 0.0080 \pm 0.0123$	$0.2523 \pm 0.0086 \pm 0.0132$	1.0218 ± 0.0162	1.0763 ± 0.0008
10.9365	$0.2375 \pm 0.0182 \pm 0.0089$	$0.2556 \pm 0.0196 \pm 0.0095$	1.0239 ± 0.0147	1.0762 ± 0.0008
10.9386	$0.2214 \pm 0.0173 \pm 0.0089$	$0.2383 \pm 0.0186 \pm 0.0095$	1.0245 ± 0.0152	1.0762 ± 0.0008
10.9400	$0.2386 \pm 0.0084 \pm 0.0124$	$0.2568 \pm 0.0090 \pm 0.0133$	1.0242 ± 0.0171	1.0762 ± 0.0008
10.9444	$0.2329 \pm 0.0082 \pm 0.0129$	$0.2507 \pm 0.0088 \pm 0.0138$	1.0208 ± 0.0171	1.0761 ± 0.0008
10.9456	$0.2177 \pm 0.0179 \pm 0.0084$	$0.2343 \pm 0.0193 \pm 0.0090$	1.0214 ± 0.0181	1.0761 ± 0.0008

\sqrt{s} (GeV)	R_b^B	R_b^{dre}	$1/(1 + \delta)$	$1/ 1 - \Pi ^2$
10.9493	$0.2346 \pm 0.0080 \pm 0.0119$	$0.2525 \pm 0.0086 \pm 0.0128$	1.0276 ± 0.0166	1.0761 ± 0.0008
10.9501	$0.2125 \pm 0.0173 \pm 0.0080$	$0.2286 \pm 0.0186 \pm 0.0086$	1.0294 ± 0.0158	1.0760 ± 0.0008
10.9536	$0.2382 \pm 0.0189 \pm 0.0090$	$0.2563 \pm 0.0203 \pm 0.0096$	1.0354 ± 0.0172	1.0760 ± 0.0008
10.9537	$0.2328 \pm 0.0083 \pm 0.0118$	$0.2505 \pm 0.0089 \pm 0.0127$	1.0358 ± 0.0173	1.0760 ± 0.0008
10.9576	$0.2163 \pm 0.0176 \pm 0.0077$	$0.2327 \pm 0.0190 \pm 0.0083$	1.0388 ± 0.0154	1.0759 ± 0.0008
10.9590	$0.2377 \pm 0.0080 \pm 0.0138$	$0.2557 \pm 0.0086 \pm 0.0149$	1.0356 ± 0.0149	1.0759 ± 0.0008
10.9633	$0.2274 \pm 0.0078 \pm 0.0126$	$0.2447 \pm 0.0084 \pm 0.0136$	1.0456 ± 0.0139	1.0758 ± 0.0008
10.9641	$0.2206 \pm 0.0085 \pm 0.0086$	$0.2373 \pm 0.0091 \pm 0.0092$	1.0495 ± 0.0136	1.0758 ± 0.0008
10.9674	$0.2236 \pm 0.0078 \pm 0.0116$	$0.2405 \pm 0.0084 \pm 0.0125$	1.0459 ± 0.0154	1.0758 ± 0.0008
10.9686	$0.2613 \pm 0.0196 \pm 0.0091$	$0.2811 \pm 0.0211 \pm 0.0098$	1.0443 ± 0.0166	1.0757 ± 0.0008
10.9726	$0.2036 \pm 0.0174 \pm 0.0072$	$0.2190 \pm 0.0187 \pm 0.0078$	1.0578 ± 0.0143	1.0756 ± 0.0008
10.9727	$0.2345 \pm 0.0078 \pm 0.0123$	$0.2522 \pm 0.0084 \pm 0.0132$	1.0579 ± 0.0139	1.0756 ± 0.0008
10.9773	$0.2441 \pm 0.0078 \pm 0.0123$	$0.2625 \pm 0.0084 \pm 0.0132$	1.0750 ± 0.0114	1.0755 ± 0.0008
10.9775	$0.2444 \pm 0.0028 \pm 0.0113$	$0.2629 \pm 0.0030 \pm 0.0122$	1.0784 ± 0.0113	1.0755 ± 0.0008
10.9791	$0.2469 \pm 0.0087 \pm 0.0086$	$0.2655 \pm 0.0093 \pm 0.0093$	1.1028 ± 0.0116	1.0754 ± 0.0008
10.9833	$0.2681 \pm 0.0084 \pm 0.0123$	$0.2883 \pm 0.0090 \pm 0.0132$	1.1385 ± 0.0123	1.0753 ± 0.0008
10.9836	$0.3097 \pm 0.0208 \pm 0.0106$	$0.3331 \pm 0.0223 \pm 0.0114$	1.1408 ± 0.0126	1.0753 ± 0.0008
10.9873	$0.2927 \pm 0.0081 \pm 0.0133$	$0.3148 \pm 0.0087 \pm 0.0144$	1.1747 ± 0.0097	1.0753 ± 0.0008
10.9901	$0.3184 \pm 0.0206 \pm 0.0104$	$0.3424 \pm 0.0221 \pm 0.0112$	1.1936 ± 0.0101	1.0752 ± 0.0008
10.9919	$0.3344 \pm 0.0034 \pm 0.0121$	$0.3595 \pm 0.0037 \pm 0.0130$	1.2094 ± 0.0101	1.0752 ± 0.0008
10.9927	$0.3523 \pm 0.0084 \pm 0.0141$	$0.3788 \pm 0.0090 \pm 0.0152$	1.2200 ± 0.0082	1.0752 ± 0.0008
10.9936	$0.3883 \pm 0.0195 \pm 0.0124$	$0.4175 \pm 0.0209 \pm 0.0133$	1.2308 ± 0.0068	1.0752 ± 0.0008
10.9975	$0.3853 \pm 0.0089 \pm 0.0139$	$0.4143 \pm 0.0095 \pm 0.0149$	1.2700 ± 0.0063	1.0752 ± 0.0008
10.9991	$0.4450 \pm 0.0101 \pm 0.0143$	$0.4785 \pm 0.0108 \pm 0.0154$	1.2785 ± 0.0068	1.0753 ± 0.0008
11.0013	$0.4512 \pm 0.0092 \pm 0.0136$	$0.4852 \pm 0.0099 \pm 0.0147$	1.2880 ± 0.0053	1.0754 ± 0.0008
11.0041	$0.5033 \pm 0.0109 \pm 0.0152$	$0.5413 \pm 0.0117 \pm 0.0164$	1.2914 ± 0.0043	1.0755 ± 0.0008
11.0068	$0.4808 \pm 0.0028 \pm 0.0135$	$0.5171 \pm 0.0030 \pm 0.0145$	1.2940 ± 0.0048	1.0756 ± 0.0008
11.0069	$0.4848 \pm 0.0089 \pm 0.0144$	$0.5215 \pm 0.0096 \pm 0.0154$	1.2935 ± 0.0048	1.0757 ± 0.0008
11.0086	$0.4884 \pm 0.0097 \pm 0.0138$	$0.5254 \pm 0.0104 \pm 0.0148$	1.2901 ± 0.0051	1.0758 ± 0.0008
11.0121	$0.4962 \pm 0.0098 \pm 0.0143$	$0.5339 \pm 0.0105 \pm 0.0154$	1.2823 ± 0.0067	1.0759 ± 0.0008
11.0151	$0.5246 \pm 0.0236 \pm 0.0149$	$0.5645 \pm 0.0254 \pm 0.0160$	1.2729 ± 0.0063	1.0761 ± 0.0008
11.0164	$0.4900 \pm 0.0033 \pm 0.0130$	$0.5274 \pm 0.0036 \pm 0.0140$	1.2659 ± 0.0059	1.0762 ± 0.0008
11.0188	$0.4662 \pm 0.0093 \pm 0.0147$	$0.5018 \pm 0.0100 \pm 0.0159$	1.2456 ± 0.0047	1.0763 ± 0.0008
11.0191	$0.4761 \pm 0.0094 \pm 0.0131$	$0.5125 \pm 0.0101 \pm 0.0141$	1.2423 ± 0.0049	1.0763 ± 0.0008
11.0214	$0.4621 \pm 0.0095 \pm 0.0137$	$0.4974 \pm 0.0102 \pm 0.0147$	1.2195 ± 0.0061	1.0764 ± 0.0008
11.0220	$0.4508 \pm 0.0030 \pm 0.0124$	$0.4852 \pm 0.0032 \pm 0.0133$	1.2184 ± 0.0058	1.0764 ± 0.0008
11.0241	$0.4253 \pm 0.0096 \pm 0.0136$	$0.4579 \pm 0.0103 \pm 0.0146$	1.2098 ± 0.0086	1.0764 ± 0.0008
11.0266	$0.4254 \pm 0.0215 \pm 0.0133$	$0.4579 \pm 0.0231 \pm 0.0143$	1.1998 ± 0.0084	1.0764 ± 0.0008
11.0269	$0.4425 \pm 0.0093 \pm 0.0134$	$0.4763 \pm 0.0100 \pm 0.0144$	1.1998 ± 0.0077	1.0764 ± 0.0008
11.0313	$0.4161 \pm 0.0101 \pm 0.0133$	$0.4479 \pm 0.0109 \pm 0.0143$	1.1912 ± 0.0120	1.0765 ± 0.0008
11.0331	$0.4199 \pm 0.0200 \pm 0.0128$	$0.4520 \pm 0.0215 \pm 0.0138$	1.1813 ± 0.0064	1.0765 ± 0.0008
11.0386	$0.3870 \pm 0.0089 \pm 0.0132$	$0.4166 \pm 0.0096 \pm 0.0142$	1.1593 ± 0.0087	1.0766 ± 0.0008
11.0401	$0.3947 \pm 0.0198 \pm 0.0131$	$0.4250 \pm 0.0213 \pm 0.0141$	1.1589 ± 0.0078	1.0766 ± 0.0008
11.0402	$0.3815 \pm 0.0087 \pm 0.0132$	$0.4107 \pm 0.0093 \pm 0.0143$	1.1584 ± 0.0079	1.0766 ± 0.0008

\sqrt{s} (GeV)	R_b^B	R_b^{dre}	$1/(1 + \delta)$	$1/ 1 - \Pi ^2$
11.0446	$0.3528 \pm 0.0198 \pm 0.0123$	$0.3799 \pm 0.0213 \pm 0.0132$	1.1490 ± 0.0102	1.0766 ± 0.0008
11.0474	$0.3720 \pm 0.0090 \pm 0.0111$	$0.4004 \pm 0.0097 \pm 0.0120$	1.1381 ± 0.0127	1.0766 ± 0.0008
11.0491	$0.4037 \pm 0.0215 \pm 0.0146$	$0.4346 \pm 0.0231 \pm 0.0157$	1.1355 ± 0.0140	1.0766 ± 0.0008
11.0531	$0.3185 \pm 0.0200 \pm 0.0124$	$0.3429 \pm 0.0216 \pm 0.0133$	1.1315 ± 0.0160	1.0765 ± 0.0008
11.0581	$0.3572 \pm 0.0194 \pm 0.0139$	$0.3845 \pm 0.0209 \pm 0.0149$	1.1228 ± 0.0149	1.0765 ± 0.0008
11.0636	$0.3374 \pm 0.0188 \pm 0.0139$	$0.3632 \pm 0.0202 \pm 0.0149$	1.1193 ± 0.0163	1.0765 ± 0.0008
11.0686	$0.3265 \pm 0.0196 \pm 0.0136$	$0.3515 \pm 0.0211 \pm 0.0146$	1.1182 ± 0.0154	1.0765 ± 0.0008
11.0721	$0.3545 \pm 0.0198 \pm 0.0136$	$0.3816 \pm 0.0213 \pm 0.0147$	1.1179 ± 0.0142	1.0765 ± 0.0008
11.0787	$0.3238 \pm 0.0182 \pm 0.0132$	$0.3486 \pm 0.0195 \pm 0.0142$	1.1225 ± 0.0139	1.0764 ± 0.0008
11.0827	$0.3324 \pm 0.0166 \pm 0.0131$	$0.3578 \pm 0.0178 \pm 0.0141$	1.1262 ± 0.0142	1.0764 ± 0.0008
11.0877	$0.3466 \pm 0.0201 \pm 0.0131$	$0.3731 \pm 0.0216 \pm 0.0141$	1.1254 ± 0.0135	1.0764 ± 0.0008
11.0932	$0.3593 \pm 0.0201 \pm 0.0130$	$0.3868 \pm 0.0217 \pm 0.0140$	1.1296 ± 0.0143	1.0764 ± 0.0008
11.0982	$0.3286 \pm 0.0196 \pm 0.0127$	$0.3537 \pm 0.0211 \pm 0.0137$	1.1245 ± 0.0127	1.0765 ± 0.0008
11.1012	$0.3368 \pm 0.0191 \pm 0.0127$	$0.3626 \pm 0.0206 \pm 0.0137$	1.1186 ± 0.0121	1.0765 ± 0.0008
11.1077	$0.3366 \pm 0.0090 \pm 0.0126$	$0.3623 \pm 0.0097 \pm 0.0136$	1.1144 ± 0.0125	1.0764 ± 0.0008
11.1092	$0.2959 \pm 0.0193 \pm 0.0113$	$0.3186 \pm 0.0208 \pm 0.0121$	1.1151 ± 0.0131	1.0764 ± 0.0008
11.1112	$0.3445 \pm 0.0188 \pm 0.0126$	$0.3709 \pm 0.0202 \pm 0.0136$	1.1190 ± 0.0134	1.0764 ± 0.0008
11.1162	$0.3463 \pm 0.0188 \pm 0.0126$	$0.3728 \pm 0.0202 \pm 0.0135$	1.1289 ± 0.0171	1.0764 ± 0.0008
11.1217	$0.3505 \pm 0.0210 \pm 0.0126$	$0.3773 \pm 0.0227 \pm 0.0135$	1.1412 ± 0.0233	1.0764 ± 0.0008
11.1262	$0.3547 \pm 0.0564 \pm 0.0125$	$0.3819 \pm 0.0608 \pm 0.0134$	1.1292 ± 0.0192	1.0765 ± 0.0008
11.1277	$0.3472 \pm 0.0202 \pm 0.0125$	$0.3737 \pm 0.0217 \pm 0.0134$	1.1266 ± 0.0178	1.0765 ± 0.0008
11.1327	$0.3315 \pm 0.0190 \pm 0.0124$	$0.3568 \pm 0.0205 \pm 0.0134$	1.1266 ± 0.0150	1.0765 ± 0.0008
11.1347	$0.3343 \pm 0.0195 \pm 0.0124$	$0.3599 \pm 0.0210 \pm 0.0134$	1.1303 ± 0.0124	1.0765 ± 0.0008
11.1432	$0.3591 \pm 0.0203 \pm 0.0136$	$0.3865 \pm 0.0219 \pm 0.0146$	1.1286 ± 0.0151	1.0765 ± 0.0008
11.1467	$0.3549 \pm 0.0199 \pm 0.0124$	$0.3820 \pm 0.0214 \pm 0.0134$	1.1337 ± 0.0126	1.0765 ± 0.0008
11.1497	$0.3403 \pm 0.0187 \pm 0.0124$	$0.3663 \pm 0.0201 \pm 0.0133$	1.1367 ± 0.0137	1.0765 ± 0.0008
11.1552	$0.3434 \pm 0.0196 \pm 0.0123$	$0.3696 \pm 0.0211 \pm 0.0132$	1.1255 ± 0.0137	1.0765 ± 0.0008
11.1582	$0.3777 \pm 0.0280 \pm 0.0135$	$0.4067 \pm 0.0301 \pm 0.0146$	1.1222 ± 0.0139	1.0765 ± 0.0008
11.1607	$0.3166 \pm 0.0272 \pm 0.0122$	$0.3408 \pm 0.0293 \pm 0.0132$	1.1206 ± 0.0158	1.0765 ± 0.0008
11.1677	$0.3221 \pm 0.0200 \pm 0.0123$	$0.3467 \pm 0.0216 \pm 0.0132$	1.1247 ± 0.0134	1.0765 ± 0.0008
11.1697	$0.3569 \pm 0.0196 \pm 0.0135$	$0.3842 \pm 0.0211 \pm 0.0145$	1.1231 ± 0.0114	1.0765 ± 0.0008
11.1787	$0.3760 \pm 0.0197 \pm 0.0135$	$0.4047 \pm 0.0212 \pm 0.0146$	1.1220 ± 0.0126	1.0765 ± 0.0008
11.1812	$0.3146 \pm 0.0182 \pm 0.0122$	$0.3387 \pm 0.0196 \pm 0.0131$	1.1214 ± 0.0121	1.0765 ± 0.0008
11.1847	$0.3454 \pm 0.0196 \pm 0.0134$	$0.3719 \pm 0.0210 \pm 0.0144$	1.1188 ± 0.0123	1.0765 ± 0.0008
11.1912	$0.3437 \pm 0.0195 \pm 0.0133$	$0.3700 \pm 0.0210 \pm 0.0144$	1.1224 ± 0.0111	1.0765 ± 0.0008
11.1942	$0.3257 \pm 0.0182 \pm 0.0122$	$0.3507 \pm 0.0196 \pm 0.0131$	1.1258 ± 0.0115	1.0765 ± 0.0008
11.2017	$0.3687 \pm 0.0204 \pm 0.0134$	$0.3969 \pm 0.0219 \pm 0.0144$	1.1314 ± 0.0160	1.0765 ± 0.0008
11.2062	$0.3567 \pm 0.0219 \pm 0.0133$	$0.3840 \pm 0.0236 \pm 0.0144$	1.1354 ± 0.0191	1.0765 ± 0.0008